

Asteroid Family Physical Properties

Joseph R. Masiero

NASA Jet Propulsion Laboratory/Caltech

Francesca DeMeo

Harvard/Smithsonian Center for Astrophysics

Toshihiro Kasuga

Planetary Exploration Research Center, Chiba Institute of Technology

Alex H. Parker

Southwest Research Institute

An asteroid family is typically formed when a larger parent body undergoes a catastrophic collisional disruption, and as such family members are expected to show physical properties that closely trace the composition and mineralogical evolution of the parent. Recently a number of new datasets have been released that probe the physical properties of a large number of asteroids, many of which are members of identified families. We review these data sets and the composite properties of asteroid families derived from this plethora of new data. We also discuss the limitations of the current data, and the open questions in the field.

1. INTRODUCTION

Asteroid families provide waypoints along the path of dynamical evolution of the solar system, as well as laboratories for studying the massive impacts that were common during terrestrial planet formation. Catastrophic disruptions shattered these asteroids, leaving swarms of bodies behind that evolved dynamically under gravitational perturbations and the Yarkovsky effect to their present-day locations, both in the Main Belt and beyond. The forces of the family-forming impact and the gravitational reaccumulation of the collisional products also left imprints on the shapes, sizes, spins, and densities of the resultant family members (see chapter by *Michel et al.*, in this volume). By studying the physical properties of the collisional remnants, we can probe the composition of the parent asteroids, important source regions of transient populations like the near-Earth objects, and the physical processes that asteroids are subjected to on million- and billion-year timescales.

In the thirteen years since the publication of *Asteroids III*, research programs and sky surveys have produced physical observations for nearly two orders of magnitude more asteroids than were previously available. The majority of these characterized asteroids are members of the Main Belt, and approximately one third of all known Main Belt asteroids (MBAs) with sizes larger than a few kilometers can be associated with asteroid families. As such, these data sets represent a windfall of family physical property information, enabling new studies of asteroid family formation and evolution. These data also provide a feedback mechanism for dynamical analyses of families, particularly age-dating

techniques that rely on simulating the non-gravitational forces that depend on an asteroid's albedo, diameter, and density.

In *Asteroids III*, *Zappalà et al.* (2002) and *Cellino et al.* (2002) reviewed the physical and spectral properties (respectively) of asteroid families known at that time. *Zappalà et al.* (2002) primarily dealt with asteroid size distributions inferred from a combination of observed absolute H magnitudes and albedo assumptions based on the subset of the family members with well-measured values. Surveys in the subsequent years have expanded the number of measured diameters and albedos by nearly two orders of magnitude, allowing for more accurate analysis of these families. *Cellino et al.* (2002) discussed the spectroscopic properties of the major asteroid families known at that time. The principal leap forward since *Asteroids III* in the realm of spectroscopy has been the expansion of spectroscopic characterization to near-infrared (NIR) wavelengths. The development of more sensitive instrumentation covering the 1 μm and 2 μm silicate absorption features and new observing campaigns to acquire NIR spectra for a large number of objects have revolutionized studies of asteroid composition and space weathering.

By greatly expanding the number of family members with measured physical properties, new investigations of asteroid families can be undertaken. Measurements of colors and albedo allow us to identify outliers in our population lists and search for variations in surface properties of family members that might indicate heterogeneity of the parent body or weathering processes. Diameter measurements

let us build a size frequency distribution and estimate the original parent body size, both of which are critical to probing the physics of giant impacts. Spectra provide detailed mineralogical constraints of family members, allowing for more sensitive tests of space weathering and parent heterogeneity, albeit for a smaller sample size, while also probing the formation environment and allowing for comparisons to meteorite samples.

In this chapter, we highlight the datasets that have been obtained since Asteroids III which have greatly expanded our ability to understand asteroid families. We discuss their implications for specific families, and tabulate average photometric, albedo, and spectroscopic properties for 109 families identified in the chapter by Nesvorný *et al.* in this volume. We also discuss the key questions that have been answered since Asteroids III, the ones that remain open, and the new puzzles that have appeared over the last decade.

2. NEW DATA SETS

The field of asteroid research has benefited in the last 13 years from a huge influx of data. Many of these large sets of asteroid characterization data (including photometric and thermophysical data) have been ancillary results of surveys primarily designed to investigate astrophysical sources beyond the solar system. Simultaneously, observing programs designed to acquire more time-intensive data products such as asteroid spectra, photometric light curves, or polarimetric phase curves have also blossomed. We review below the main datasets that have advanced family characterization in recent years.

2.1 Optical colors from SDSS

The Sloan Digital Sky Survey (SDSS, York *et al.* 2000) produced one of the first extremely large, homogeneous data sets that contained information about asteroid surface properties at optical wavelengths. These data are archived in the SDSS Moving Object Catalog (<http://www.astro.washington.edu/users/ivezic/sdssmoc/sdssmoc.html>) which currently contains 471,569 entries of moving objects from survey scans conducted up to March 2007. The catalog entries can be associated with 104,449 unique known moving objects, however $\sim 250,000$ entries do not have corresponding associations in the orbital element catalogs implying the potential for a significant benefit from future data mining efforts.

While the SDSS 5-color photometric system (u, g, r, i, z , with central wavelengths of 0.3543 μm , 0.4770 μm , 0.6231 μm , 0.7625 μm , 0.9134 μm , respectively) was not designed with asteroid taxonomy in mind (unlike previous surveys such as the Eight Color Asteroid Survey, Zellner *et al.* 1985a), the sheer size of the dataset coupled with its extremely well-characterized performance has made SDSS an immensely valuable asset for defining asteroid families and exploring their properties. The near-simultaneous optical

color information obtained during the course of the SDSS survey can be used to infer the spectroscopic properties of tens of thousands of asteroids at optical wavelengths.

The Sloan Digital Sky Survey, primarily designed to measure the redshifts of a very large sample of galaxies, serendipitously observed many asteroids over the course of its several survey iterations. Under standard survey operations with 53.9 second exposures, its five-color camera was sensitive to stationary sources as faint as $r \sim 22.2$, with similar performance in u and g and somewhat brighter limits in i and z (21.3 and 20.5, respectively). To enable the accurate determination of photometric redshifts, high-precision internal and absolute calibrations were essential. The care and effort expended on these calibrations carried over into the dataset of moving object photometry, resulting in the largest well-calibrated dataset of multi-band asteroid photometry to date.

As of the latest data release, the Moving Object Catalog 4 (MOC4, Parker *et al.* 2008) contains asteroid observations from 519 survey observing runs. The automatic flagging and analysis of moving objects required that they be brighter than magnitude $r = 21.5$. The brightest object in the sample is $r \sim 12.91$, giving the survey a dynamic range of over 8.5 magnitudes. The large sample size and dynamic range of this survey make it a powerful tool for studying luminosity functions of dynamically- or photometrically-selected sub-populations of the moving objects, of which asteroid families are a natural example.

Because of the much smaller sample size of asteroids with u -band observations having photometric errors < 0.1 mag (44,737, compared with 442,743 with a similar precision in r -band), most large-scale asteroid studies using the SDSS photometry have considered only the four longer-wavelength bands. These are often further collapsed into two principle components, the a^* color ($a^* = 0.89(g - r) + 0.45(r - i) - 0.57$) and the $(i - z)$ color (see Ivezić *et al.* 2001).

Using the SDSS data set, Ivezić *et al.* (2002) showed that asteroid families are easily identified from their optical colors. They found four primary color classes of families which describe one of four characteristic compositions: Vesta, Koronis, Eos, and Themis. Jedicke *et al.* (2004) and Nesvorný *et al.* (2005) expanded upon this to investigate space weathering and find that older asteroid families have steeper spectral slopes from 0.55 to 1 micron than younger asteroid families.

Szabó & Kiss (2008) used SDSS photometry to constrain the shape distributions of eight large asteroid families. By assuming the observed magnitude differences between different epochs of observation were uncorrelated, they showed that both older families and families closer to the Sun tend to have more spherical shape distributions. This effect is what would be expected for a system where small-scale cratering collisions redistributed material into gravitational lows, resulting in a more spherical shape.

Parker *et al.* (2008) used the family color relationships found by Ivezić *et al.* (2002) as a springboard to refine

the definition of asteroid families beyond solely dynamical relationships. The ability to spectrophotometrically-refine the sample of objects linked to each family meant family membership could be extended further into the background, and allowed the identification of diffuse family “halos” of compositionally-distinct objects (*Parker et al.* 2008, *Brož & Morbidelli* 2013, *Carruba et al.* 2013). Overlapping but compositionally-distinct families such as Flora and Baptistina are easily separated with the addition of color information.

Using the wealth of SDSS data, *Carvano et al.* (2010) modeled established taxonomic classes to define the SDSS color parameters of each class. They then used these constraints to perform photometric taxonomic classifications of SDSS-observed asteroids, including many large asteroid families. This technique was later extended by *DeMeo & Carry* (2013) to better distinguish the boundaries between taxonomic classes. This taxonomic strategy can be applied to future photometric surveys to rapidly classify asteroids as a tool for improving family associations. While the resulting taxonomic grouping is of lower certainty than spectroscopic classification, spectrophotometric taxonomy offers a fast way to quantify the spectral behavior of large numbers of asteroids and provide high-quality candidates for spectroscopic followup.

2.2 Visible and IR Spectroscopic Surveys

Spectroscopic measurements provide unparalleled sensitivity to the mineralogical features on the surfaces of asteroids. As members of families come from the same progenitor object, surveys of many family members allow us to probe the composition of that parent body and search for mineralogical changes indicative of geological processes during the parent’s formation and early evolution. For families shown to have homogeneous spectral properties, these surveys can also be used to identify outlier objects that are compositionally distinct from the family, especially large objects that can present serious complications to the analysis of family evolution.

A major focus in the study of families has been the characterization of the effects of space weathering on the surfaces of atmosphereless bodies. Recent work using dynamical simulations to determine the ages of asteroid families (see the chapter by *Nesvorný et al.* in this volume for a discussion of these works) has opened a new avenue into investigating the potential effects of space weathering on asteroid surfaces. Assuming that the family-forming impact completely refreshed the surfaces of family members, we can look for families with similar compositions but different ages to search for spectral changes that would be the hallmark of space weathering. A number of researchers have conducted spectroscopic surveys of families to this end, although the results of these studies have been somewhat conflicting (e.g. *Nesvorný et al.* 2005, *Willman et al.* 2008, *Vernazza et al.* 2009, *Thomas et al.* 2011, *Thomas et al.* 2012).

Shortly after the publication of Asteroids III, large scale visible wavelength (0.45-0.9 microns) spectral surveys were published that were major driver of asteroid compositional studies. *Bus & Binzel* (2002) and *Lazzaro et al.* (2004) published 1341 and 820 asteroid spectra, respectively, providing a wealth of data for asteroid studies. Also around this time near-infrared spectrometers became widely available, such as SpeX on the NASA IRTF (*Rayner et al.* 2003). The near-infrared provides wavelength coverage that allows better characterization of silicate features (*Burbine & Binzel* 2002, *Gaffey et al.* 1993). While no single large observing campaign has been initiated for main belt asteroids in the near-infrared, many small programs have been carried out that targeted specific asteroid families (*Sunshine et al.* 2004; *Mothe-Diniz et al.* 2005; *Vernazza et al.* 2006; *Mothe-Diniz et al.* 2008a; *Mothe-Diniz & Nesvorný* 2008b; *Mothe-Diniz & Nesvorný* 2008c; *Willman et al.* 2008; *Harris et al.* 2009; *Reddy et al.* 2009; *de Sanctis et al.* 2011; *Reddy et al.* 2011; *Ziffer et al.* 2011; *de Leon et al.* 2012). A compilation of spectral taxonomic classifications of asteroids is given in the Planetary Data System by *Neese* (2010) and is periodically updated. We highlight here some of the specific families that were the subject of spectral investigations.

Vernazza et al. (2006) obtained spectra of Karin family members, finding them to be very similar to OC meteorites. *Willman et al.* (2008, 2010) extended this survey in an attempt to constrain space weathering rates for asteroid surfaces, finding that spectral slopes are altered on the billion year timescale. *Harris et al.* (2009) surveyed the Karin family using thermal infrared spectroscopy, and found albedos lower than expected for fresh asteroid surfaces, implying space weathering alters albedos on the million year timescale, in conflict with the *Willman et al.* results.

Nathues (2010) used visible and NIR spectroscopy of 97 Eunomia family members to study the potential differentiation history of the family parent. They show that the majority of family members have S-type taxonomy and the parent body was likely not fully differentiated, but may have undergone partial differentiation. *Fieber-Beyer et al.* (2011) obtained NIR spectroscopy of 12 Maria family members. From these data they associate this family with mesosiderite-type meteorites, a type iron-rich meteorite thought to originate from a differentiated parent body.

Ziffer et al. (2011) obtained NIR spectra of 13 asteroids in the Themis and Veritas families and find distinct differences in the spectral behavior of the two families. They associate both families with CM2 chondrites, but find no evidence for space weathering of C-type objects.

Reddy et al. (2009,2011) performed a spectroscopic survey of the Baptistina family aimed at constraining the composition of the family members. They found a range of compositions represented, but smaller objects as well as (298) Baptistina itself show clear association with LL-type ordinary chondrites. Ordinary chondrite meteorites show two distinct compositional phases, one at albedos similar

to S-complex asteroids and one that is darker with muted silicate absorption bands. This darker material has been associated with former surface regolith which had gases implanted by the solar wind and was later re-lithified and impact-shocked, resulting in a significantly different reflectivity with only a nominal difference in composition (Britt & Pieters, 1991). Studies of the recent Chelyabinsk meteorite (Kohout et al. 2014, Reddy et al. 2014) further confirm that shock-darkening may play a critical role in the evolution of asteroid family spectra (cf. Cellino et al., 2002).

Licandro et al. (2012) used the Spitzer space telescope to measure mid-infrared spectra for eight members of the Themis family, and determined their albedos and diameters. They were also able to constrain the surface thermal inertia and set limits on the surface composition, showing that family members must have a very low surface density.

Jasmin et al. (2013) performed a spectroscopic survey of objects classified as Qp in the SDSS spectrophotometric system in the Vesta family, but were not able to find any significant differences between these objects and canonical V-type asteroid spectra. This highlights the potential ambiguities in spectrophotometric taxonomic classifications, and the need for further spectroscopic followup of interesting asteroids to confirm their spectral behavior.

Recently, Vernazza et al. (2014) mineralogically analyzed spectra of six S-complex asteroid families and 83 background S-type objects and compared these results to compositions of various ordinary chondrite meteorites. They found a bimodality in their olivine/pyroxene mineral diagnostic for S-type asteroids which traces the compositional gradients measured for metamorphosed meteorites with a range of iron contents. This bimodality also extended to families, with Koronis, Agnia, Merxia, and Gefion more closely matching high-iron ordinary chondrites and Eunomia and Flora matching either low-iron chondrites from the interiors of bodies or ordinary chondrites from the near-surface regions showing little metamorphism. Mineralogical assessment of near-infrared spectra thus offers a new method of probing the compositions and metamorphic histories of these S-complex families.

2.3 Infrared Space Surveys

Recent improvements in mid-infrared detector technology have spurred renewed interest in their use for astronomical observations. Ground-based thermal infrared detectors can obtain data for a small subset of the brightest targets, however the thermal background prohibits large-scale surveys of smaller asteroids. The space environment, however, is ideal for thermal infrared surveys of the sky, and two recent satellites have obtained all-sky survey data at mid-infrared wavelengths of a large number of asteroids. A more complete discussion of these surveys is presented in the chapter by Mainzer et al. in this volume, and so here we only highlight a few relevant aspects.

The AKARI space telescope was launched on 21 Feb 2006 and surveyed the sky at two thermal infrared wave-

lengths from 6 May 2006 until the telescope-cooling liquid helium was exhausted on 28 August 2007, covering over 96% of the sky (Murakami et al. 2007, Ishihara et al. 2010). The “Asteroid Catalog Using AKARI” (AcuA, Usui et al. 2011, <http://darts.jaxa.jp/ir/akari/catalogue/AcuA.html>) database summarizes the asteroid survey data. Using the Standard Thermal Model (Lebofsky et al. 1986, Lebofsky & Spencer 1989), diameters and visible albedos were derived for 5120 asteroids.

AKARI also performed spectroscopic observations of 70 asteroids during the warm mission phase after the cryogen was exhausted, many of which are the largest members of asteroid families. These observations provide unique spectroscopic data covering the wavelength range from 2–5 μm (Usui et al., 2011; Usui et al., 2015, in preparation). Kasuga et al. (2012) present physical properties of Cybele family members determined from this dataset, and discuss the taxonomic composition of this family by combining spectrally derived taxonomy with infrared photometry.

The Near-Earth Object Wide-field Infrared Survey Explorer (NEOWISE) mission launched on 14 December 2009 and surveyed the entire sky at four infrared wavelengths over the course of its cryogenic mission. The survey continued during its post-cryogenic and reactivated missions at the two shortest wavelengths. The NEOWISE data catalogs and images are publicly archived at the NASA/IPAC Infrared Science Archive (<http://irsa.ipac.caltech.edu/Missions/wise.html>) and contain thermal infrared measurements of over 150,000 asteroids (Mainzer et al., 2011, 2014). Many of these were identified as members of asteroid families, allowing for the determination of diameter and albedo distributions for an unprecedented number of families.

Masiero et al. (2011) presented albedos and diameters for over 120,000 Main Belt asteroids, including over 32,000 members of 46 families from Nesvorný (2012). They showed that the albedo distribution within a family is usually very narrow, but some families have significant contamination from background objects or show a mixing of multiple families that overlap in proper-element space. Masiero et al. (2013) split the Main Belt into distinct orbital and albedo components and showed that overlapping families such as Polana and Hertha (aka Nysa) can be distinguished easily.

Masiero et al. (2013) used the NEOWISE diameters to measure the size-frequency distribution (SFD) for 76 asteroid families that they identify in their data. The SFD can be computed as $N \propto D^\alpha$ where N is the number of objects with diameter greater than D and α is the SFD slope. They found that larger families tended to show cumulative SFD slopes that converge toward the value of $\alpha = -2.5$ as expected for a collisionally equilibrated population (Dohnanyi 1969), while smaller families have a wider dispersion. The family associated with (31) Euphrosyne has an anomalously steep SFD slope, which Carruba et al. (2014) explain as the result of a dynamical draining of the largest family fragments by the ν_6 resonance, which runs through the center

of this family in semimajor axis-inclination space.

Ali-Lagoa et al. (2013) used the NEOWISE albedo measurements to show that the Pallas family has visible and infrared albedos that are distinct from the majority of B-type asteroids. *Masiero et al.* (2014) presented the $3.4\ \mu\text{m}$ albedo distributions of 13 asteroid families. They found that the asteroid families form three distinct groupings of albedos at this wavelength. Additionally, the Eos family has unique near-infrared reflectance properties, which likely traces a mineralogy not seen elsewhere in the Main Belt.

2.4 Asteroid Light Curves and Phase Curves

Over the last decade, a number of groups have carried out surveys of asteroid light curves, many focusing on the properties of specific families. Light curve analysis from a single epoch can provide rotation periods and constraints on amplitude, while multi-epoch observations can allow for rotational pole determination, shape model fitting, searches for binarity, and detection of non-principal axis rotation. The binary fraction is an important test of formation mechanisms, while pole determination for a significant number of family members allows for constraints on YORP evolution of family spin states.

One of the key results from these lightcurve studies has been the confirmation of the YORP effect on spin poles of objects with similar ages (*Vokrouhlický et al.* 2003). The YORP mechanism results from asymmetries in the thermal re-emission of absorbed light, creating a torque on the asteroid. This can alter the rotation rate of these objects, but also is predicted to rapidly reorient the spin poles of most small objects to be perpendicular to the body's orbital plane. This will result in spin poles clustered near 0° and 180° from the orbital pole, and a spin rate distribution differing from the Maxwellian distribution that is expected for a collisionally equilibrated system. *Slivan et al.* (2003, 2008, 2009) measured light curves for 30 members of the Koronis family, showing a strongly anisotropic distribution of spin poles and a non-Maxwellian rotation rate distribution, both consistent with YORP-induced rotation changes.

Surveys of other families have come to similar conclusions: *Warner et al.* (2009) surveyed the Hungaria family asteroids and determined rotation properties for over 100 of these objects. They find a significant excess of slow-rotators, which they attribute to YORP-induced spin down, as well as a binarity fraction of 15%, similar to the NEA population. *Kryszczyńska et al.* (2012) surveyed 55 objects in the Flora family to determine their rotation periods and poles. They found that the Flora family rotation rates are non-Maxwellian, as is expected from long-term YORP evolution. *Kim et al.* (2014) determined rotation properties for 57 Maria family members, finding an excess of prograde rotation states consistent with the predictions of YORP and Yarkovsky evolution resulting in retrograde rotators moving into the 3:1 Jupiter resonance and being removed from the family.

Hanuš et al. (2011, 2013) used shape models derived from light curve inversion to study the spin pole positions of ten asteroid families. They found a clear distinction in spin pole direction, where objects at semimajor axes smaller than the largest remnant have retrograde rotations while objects at larger semimajor axes have prograde rotations, as is expected from a system evolving under the Yarkovsky effect.

Using the large amount of photometric data available from the Minor Planet Center and the AstOrb database kept by Lowell Observatory, *Oszkiewicz et al.* (2011, 2012) re-derived the photometric phase functions of all known asteroids, applying the improved H, G_1, G_2 and H, G_{12} phase equations. They find that asteroid families show statistically similar phase slope parameters and that the major taxonomic complexes can be statistically differentiated. However, these distributions overlap, significantly limiting the use of phase curve parameters for direct family or taxonomy identification. *Bowell et al.* (2014) searched the Lowell data for statistical anisotropies in the ecliptic longitude distribution of rotation poles for asteroid family members. They show that the four largest groups considered (the Flora, Vesta, and Koronis families, and the Nysa-Polana complex) have anisotropic spin longitude distributions showing an excess in the $30 - 110^\circ$ longitude range and a dearth in the $120 - 160^\circ$ longitude range, consistent with the distribution seen for the Main Belt as a whole. The authors suggest this may be due to pole reorientation by the YORP effect, but that extensive modeling is required as well as consideration of potential selection biases.

2.5 Polarimetric Surveys of Families

Measurement of the polarization of light scattered off the surface of an atmosphereless body as a function of phase angle can be used as an independent constraint on the object's albedo (*Cellino et al.*, 1999). Although the magnitude range accessible to polarimetric observations is comparable to that of NIR spectroscopy, multiple nights are required for each object to constrain the phase behavior and there are fewer available imaging polarimeters that are well-calibrated than NIR spectrometers. As such, there are fewer asteroids with measured polarimetric properties, however polarimetric studies provide unique data on asteroid surface properties that can be important for disentangling ambiguities in other characterization surveys.

Cellino et al. (2010) polarimetrically surveyed the Karin and Koronis families as an independent test of the effect of space weathering on asteroid albedo. They find no significant differences between the albedos of Karin and Koronis, implying that space weathering must act on timescales shorter than the ~ 6 million year age of the Karin family.

Cellino et al. (2014) conducted a survey of the linear polarization phase curves of Watsonia asteroid family members, searching for analogs to the unusual polarization of (234) Barbara. Barbara and the related "Barbarian" objects have unusual polarimetric properties indicative of unique

surface mineralogy and are taxonomically identified as Ld-type objects from spectra. They found that seven of the nine objects surveyed show indications of a surface rich in spinel, one of the oldest minerals in the solar system (*Burbine et al.*, 1992). This implies that the Watsonia parent object has undergone little-to-no mineralogical processing since the formation of the first solids in the protosolar disk (*Sunshine et al.*, 2008), and may have been one of the oldest unprocessed bodies in the Solar system.

3. COLOR, SPECTRA, ALBEDO, AND SIZE DISTRIBUTIONS OF FAMILIES

With the wealth of asteroid physical observations now available, we can determine the average characteristic properties for families. As the literature contains many different collections of family lists, here we focus on the consolidated list presented in the chapter by *Nesvorný et al.* in this volume. This improves our sensitivity to subtle physical differences between families, especially the biggest families where the large sample size can greatly reduce the scatter in measured properties among individual members. We can also use these data to reject outlier objects from family lists, particularly when the family of interest is of distinct composition from other nearby families or the majority of background objects. Here we discuss some of the recent applications of the new physical property data that has become available.

3.1 Homogeneity of Families and Use of Physical Properties to Distinguish Outliers

Family-forming collisions are expected to liberate material from a large fraction of the parent body's volume. Many of the resulting family members are likely to be accumulations of smaller ejecta, potentially from a range of lithologies within the parent (see the chapter by *Michel et al.* in this volume). For a heterogeneous parent body, we would expect to see a range of colors, spectra, and albedos among the resultant family members, while a homogeneous parent would instead produce a family with very narrow distributions of these properties. While it is possible that the family formed from an impact on a homogeneous parent by an impactor of a different composition could show heterogeneity, statistically the mass of any probable impactor will be only a small fraction of the mass of either the parent or the ejecta, and so would be unlikely to be a significant contaminant to globally averaged properties obtained from remote sensing. Sub-families resulting from second-generation impacts could also show subtle property differences compared to the original family due to the reset of any space weathering processes, however this would be most obvious only for very young families (e.g. *Karin*).

Early surveys of asteroid family spectra and colors indicated that with the exception of a handful of outliers (e.g.

the Nysa-Polana complex) families had narrow distributions of physical properties, indicative of homogeneous parent bodies (see *Cellino et al.*, 2002 and references therein). This enabled the extrapolation of measured physical properties for a handful of family members to the entire family. As many of the largest remnants of family formation had been studied for decades, this became a boon to family research.

However, with the availability of physical property data for large numbers of family members, we can now use this data to remove interloper objects from family lists when they have a different color, albedo, or spectrum from the bulk of the family. Refining family lists in this way is particularly important for improving the accuracy of age-dating techniques. In the past few years, a number of research groups have been actively using these data to this end, in an effort to better understand the formation and evolution of families and the parent bodies they came from (e.g. *Novaković et al.* 2011; *Brož et al.* 2013; *Masiero et al.* 2013; *Carruba* 2013; *Walsh et al.* 2013; *Carruba et al.* 2013; *Hanuš et al.* 2013; *Milani et al.* 2014).

3.2 Combined Properties of Individual Families

Using the various data sets presented above, we provide in Table 1 the average SDSS colors, average optical and NIR albedos, majority taxonomic type, and SFD slopes (as well as the diameter range that the SFD was fit to) for the families given in the chapter by *Nesvorný et al.* in this volume. We also present a visualization of the average albedo, SDSS colors and spectra for families with sufficient data in Figure 1. While mean values are often useful for extrapolating properties of family members that were not observed, or for comparing families to each other or other ground-truth data, there are important caveats that cannot be ignored. Sample size considerations and the uncertainty on individual measurements are the most critical of these caveats: average values based on a small number of objects or even a single object should be considered potentially spurious, and treated as such. We include those values here for completeness.

Visible albedo mean values were derived by fitting a Gaussian to the distribution of all measured $\log p_V$ values, following the technique *Masiero et al.* (2011) applied to the NEOWISE data, and the quoted error gives the width of the observed distribution. The uncertainty on the mean value, when comparing mean albedos of various families, will be the measured Gaussian width over the square root of the sample size; thus for large families the mean albedo can be known quite accurately, even if individuals have large uncertainties. Family NIR albedo values are a median of the 3.4 μm albedos given in *Masiero et al.* (2014).

Size frequency distributions (SFDs) were computed for all families with more than 100 measured diameters from all infrared surveys and were found by fitting a power law to the cumulative size distribution, using only those bins with more than 5 objects (to reduce the influence of the large remnants) and less than half the total sample (to minimize

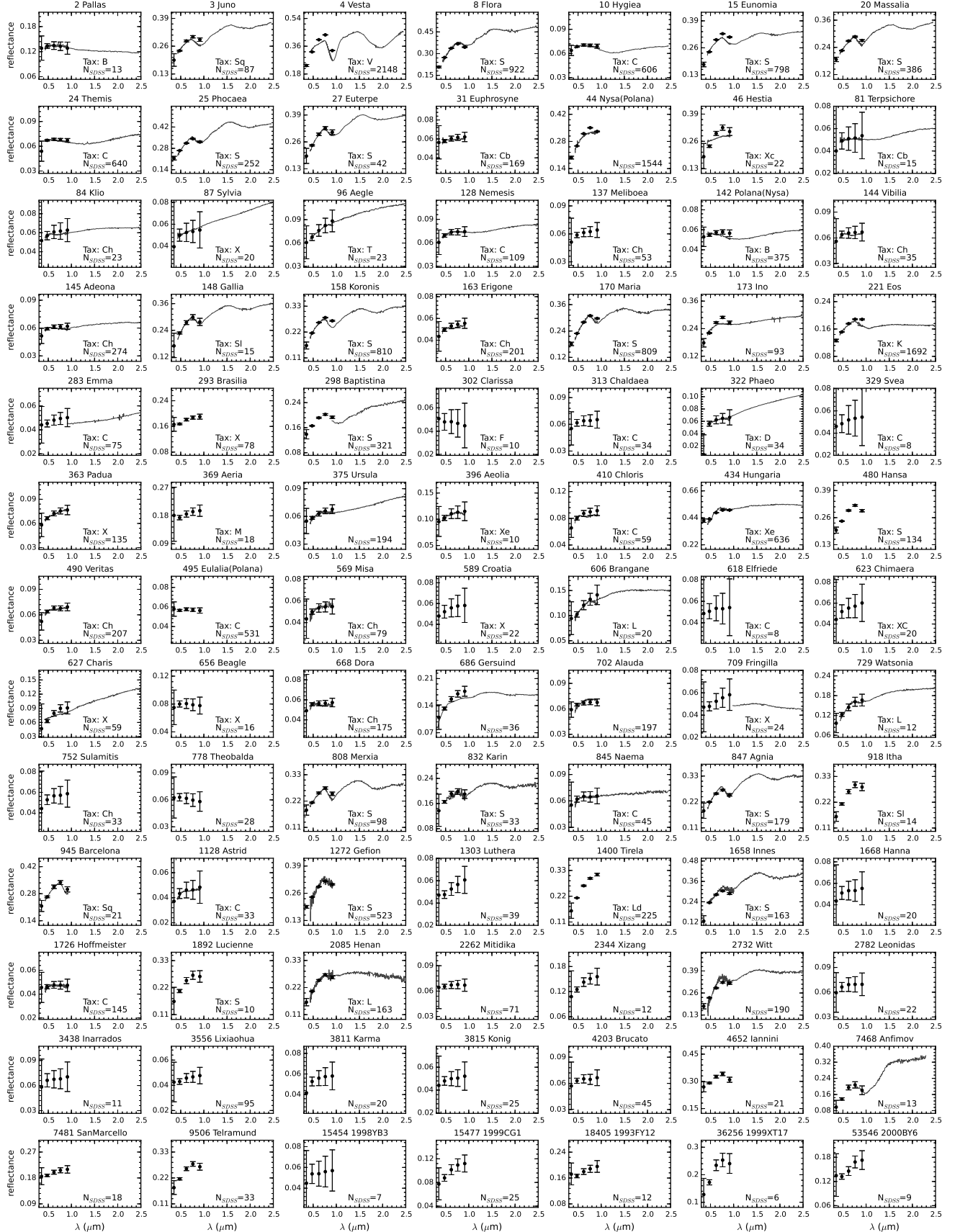


Fig. 1.— Average solar-corrected SDSS colors (points) and sample⁷ optical/NIR spectra (from SMASS) for all asteroid families listed in Table 1 with sufficient data. Plots are scaled such that the interpolated reflectance at $0.55 \mu\text{m}$ equals the average visible geometric albedo (p_V) for the family from all infrared surveys. The “N” in the bottom right of each plot indicates the number of SDSS observations used, and taxonomic class is given when available. Note the reflectance scale in each plot is different.

the effects of incomplete diameter sampling at small sizes). Tabulated SDSS colors were calculated by performing an error-weighted mean of all observations having $\text{SNR} > 10$ in the g, r, i , and z bands used to calculate a^* and $i - z$. Family taxonomy is given only for cases where a majority of family members with taxonomic classes had the same class. If no subclass (e.g. Ch, Sq, Ld) had a majority, but a majority of members were in the same complex, that complex is listed (e.g. C, S, L). For each of these parameters we include the number of objects used to compute the listed value.

Although we implicitly assume that the variation in observed properties is a result of statistical uncertainties and that all family members should have the same physical properties, this is not necessarily true. Outlier objects may be statistical flukes, or background contamination, but they just as easily may be interesting pieces of the parent body warranting further study, a determination that cannot be made or captured here. Additionally, a single mean value ignores any size-dependent effects in the data, either real or imposed by detection or sample-selection biases.

Only a proper debiasing of each survey accounting for observing geometry, detector sensitivity, and detection efficiency can determine the true value for each parameter. This is particularly important for cases of mismatched sensitivities, such as the SDSS r vs z magnitudes needed for colors or the NEOWISE W3 flux vs ground-based H_V magnitude needed for albedo determination; only objects seen in both datasets will have a measured value which strongly biases the outcome as a function of apparent brightness. Thus Table 1 is meant as a overarching guide, but caution is mandated for any interpretation of values or trends.

A number of low albedo families can only be identified when the low albedo population of the Main Belt is considered independently. This is due to the bias toward discovery of high-albedo objects by ground-based visible-light surveys. As the population of high albedo asteroids is probed to smaller sizes (and thus larger numbers) these families will overwhelm traditional HCM techniques, particularly the calculation of the quasi-random level needed to assess the reality of a given family, making low albedo families harder to identify. *Masiero et al.* (2013) circumvented this by considering each albedo component separately, and by restricting their sample to objects detected in the thermal infrared, which is albedo-independent (see the chapter by *Mainzer et al.* in this volume for further discussion). As the sample of known asteroids continues to increase, development of new techniques for the identification of asteroid families from the background population (e.g. *Milani et al.* 2014) will increase in importance.

Below we discuss individual families that merit specific mention based on recent research. We include the PDS ID number from *Nesvorný et al.* (2012) both below and in Table 1 for easier association with other work and with the family dynamical properties given in the chapter by *Nesvorný et al.* in this volume.

3.2.1 Hungaria

The Hungaria asteroid family (PDS ID 003) occupies a region of space interior to the rest of the Main Belt and with an orbital inclination above the ν_6 secular resonance. This region is an island of stability between the major resonances that dominate this area of the solar system, and likely samples a unique region of the protoplanetary disk (*Bottke et al.* 2012). *Warner et al.* (2009) analyzed light curves of 129 Hungaria asteroids, finding a significant excess of very slow rotating bodies. They also showed that the binary fraction of this population is $\sim 15\%$, comparable to the fraction seen in the NEO population.

The albedos for Hungaria family members derived from the NEOWISE data by *Masiero et al.* (2011) have values significantly larger than $p_V > 0.5$, however this is an artifact of bad absolute magnitude fits for these objects in orbital element databases, which when corrected bring the best-fit albedo values to the range of $0.4 < p_V < 0.5$ (*B. Warner*, private communication). Spectroscopic and SDSS color studies of the Hungaria family show the classification to be X-type, which when combined with the very high albedos translates to an E-type classification (*Carvano et al.* 2001; *Assandri & Gil-Hutton*, 2008; *Warner et al.* 2009). Polarimetric observations by *Gil-Hutton et al.* (2007) of the overall Hungaria region indicate inconsistencies in the polarimetric behavior of asteroids in and around the Hungaria family.

3.2.2 Flora

The Flora family (PDS ID 401) is a large S-type family residing in the inner Main Belt. The largest remnant, (8) Flora, has an orbit just exterior to the ν_6 resonance, and only the half of the family at larger semimajor axes is seen today. The ν_6 resonance is particularly good at implanting asteroids into the NEO population (*Bottke et al.* 2000), meaning that Flora family members are likely well-represented in the NEO population and meteorite collections. Recent spectroscopic observations of Flora family members have been combined with analyses of meteorite samples to link the LL chondrite meteorites to the Flora family (*Vernazza et al.* 2008; *de Leon et al.* 2010; *Dunn et al.* 2013). This provides an important ground-truth analog for interpreting physical properties of S-type objects in the Main Belt and near-Earth populations. We note that in contrast to previous analyses, *Milani et al.* (2014) did not identify a family associated with Flora, instead finding that candidate member asteroids merged with the Vesta and Massalia families, or potentially are part of their newly identified Levin family. However, the Vesta family has a distinct $i - z$ color that is not shown by Flora family members (see Table 1), making these populations easily distinguished by their photometric properties. While the Flora and Massalia populations overall have properties that are consistent within uncertainties, the difference between the mean albedos of these two populations suggests they in fact are different populations.

3.2.3 Baptistina

Over the past decade, the Baptistina family (PDS ID 403) has been the focus of a number of investigations, leading to controversy over the physical characteristics of these asteroids. Initial investigations assumed the family had characteristics similar to C-type asteroids (e.g. low albedo) based on spectra of the largest member (298) Baptistina (Bottke *et al.*, 2007). This was used in numerical simulations to show that Baptistina was a probable source of the K/T impactor. Further spectral investigations of a 16 large family members found compositions more analogous to LL chondrites, ruling out a C-type association (Reddy *et al.*, 2011). However, a major difficulty in studying this family is the significant overlap in orbital element-space with the much larger Flora family (or with the Levin family, according to Milani *et al.* (2014)), making it difficult to ensure that the spectral studies were probing Baptistina and not Flora. Using albedos to separate these families finds a mean albedo of $p_V = 0.16$, which is not consistent with either C-type or LL chondrite compositions (Masiero *et al.* 2013). Recent analysis of the Chelyabinsk meteorite samples showed that shock darkening of chondritic material could produce an albedo consistent with the Baptistina family without altering the composition (Reddy *et al.* 2014) offering a potential solution to the seemingly contradictory information about this family, but future work will be necessary to confirm this hypothesis.

3.2.4 “Nysa-Polana”

In the years leading up to Asteroids III it had become increasingly clear that Nysa-Polana, interpreted as a single entity, was likely to be a short-lived phenomenon. Cellino *et al.* (2001) presented a spectroscopic study of 22 asteroids associated with the group, and found that the group was best understood as two compositionally distinct families partly overlapping in orbital element space, one associated with the F class in the Tholen taxonomy and one with the S class, while (44) Nysa was compositionally distinct and potentially not associated with either family.

Masiero *et al.* (2011) showed that the albedo distribution of the ~ 3000 asteroids identified as part of the Nysa-Polana complex were strongly bimodal, unlike the majority of families. Although overlapping in semimajor axis-inclination space, the high- and low-albedo components occupy distinct regions of semimajor axis-eccentricity space, supporting the theory that they are two distinct populations coincidentally overlapping as opposed to a single parent body that was composed of two distinct mineralogies.

Using albedo as a discriminant, Masiero *et al.* (2013) were able to uniquely identify two separate families, a low-albedo one associated with (142) Polana, and a high-albedo one with (135) Hertha (PDS ID 405), while (44) Nysa no longer linked to either family. In Table 1 we continue to refer to the high-albedo family as “Nysa” despite the evidence to the contrary, for consistency with other literature. Walsh

et al. (2013) expanded on this, and used the family albedos to reject objects with S-type physical properties and focus on the low-albedo component of the Nysa-Polana group. Using dynamical constraints, they were able to further subdivide the low-albedo component of this group into two distinct families, which they identify as the Eulalia family and the “new Polana” family. They estimate ages for each of these families of $0.9 - 1.5$ billion years and > 2 billion years, respectively. Conversely, Milani *et al.* (2014) identify the whole complex as associated with Hertha and split this region into two components by combining dynamics and physical properties, which they identify as the Polana and Burdett families (low and high albedo, respectively).

3.2.5 Vesta

The Vesta asteroid family (PDS ID 401) has historically been one of the most well-studied families, due to its clear association with one of the largest known asteroids, the high albedos and locations in the inner Main Belt making members favorable for ground-based observations, and association with the HED meteorites leading to the interpretation of (4) Vesta as a differentiated parent body (McCord *et al.*, 1970; Zappala *et al.*, 1990; Binzel & Xu 1993; Consolmagno & Drake, 1977; Moskovitz *et al.*, 2010; Mayne *et al.*, 2011). With the recent visit of the Dawn spacecraft to (4) Vesta (see the chapter by Russell *et al.* in this volume) ground-truth data can be compared to remote-sensing observations of family members. Additionally, constraints on the ages of the major impact basins of 1.0 ± 0.2 billion years for Rheasilvia and 2.1 ± 0.2 billion years for Veneneia (Schenk *et al.* 2012) set strong constraints on the possible age of Vesta family members. Milani *et al.* (2014) find that the Vesta family splits into two subgroups in their analysis, which they attribute to these two events.

The Vesta family has a unique mineralogical composition in the Main Belt, making it easily distinguishable in color-, albedo-, or spectral-space. In particular, members stand out from all other asteroids in terms of their high albedo, low $i - z$ color, and deep $1 \mu\text{m}$ and $2 \mu\text{m}$ absorption bands. This has prompted searches for objects with similar properties at more distant locations in the Main Belt (e.g. Moskovitz *et al.* 2008; Duffard & Roig, 2009; Moskovitz *et al.*, 2010; Solonoi *et al.* 2012). These bodies could only have evolved from the Vesta family via a low-probability series of secular resonances (Carruba *et al.* 2005, Roig *et al.* 2008a), and may be indicative of other parent bodies that were differentiated. To date only a few candidate objects from these searches have been confirmed to be V-type, indicating that the collisional remnants of the other differentiated objects that must have formed in the early solar system has likely been dynamically erased.

3.2.6 Eunomia

The Eunomia family (PDS ID 502) is an old, S-type family located in the middle Main Belt. Spectral evidence

presented by *Lazzaro et al.* (1999) indicates that the Eunomia family may have originated from a partially differentiated parent body. *Natheus et al.* (2005) and *Nathues et al.* (2010) investigated the physical properties of the Eunomia largest remnant and 97 smaller family members as a probe of the composition and differentiation history of the original parent body. They found that the largest remnant shows two hemispheres with slightly different compositions that support an interpretation of the impact causing significant crust-loss and some mantle-loss on a partially-differentiated core. *Milani et al.* (2014) found two subfamilies within Eunomia, which they attribute to separate cratering events.

3.2.7 Eos

The Eos family (PDS ID 606) represents the primary reservoir of K-type asteroids in the Main Belt, and can easily be identified by their $3.4\ \mu\text{m}$ albedo (*Masiero et al.* 2014). This spectral class has been proposed as the asteroidal analog of the CO and CV carbonaceous chondrite meteorites (*Bell et al.* 1988; *Doressoundiram et al.* 1998; *Clark et al.* 2009). This would imply that the Eos family is one of the best sampled collisional families in our meteorite collection, and would mean that many of these samples do not probe the C-complex asteroids as had frequently been assumed.

Mothé-Diniz & Carvano (2005) compared spectra of (221) Eos with meteorite samples and inferred that the Eos parent body likely underwent partial differentiation. *Mothé-Diniz et al.* (2008a) extended this work to 30 Eos family members and found mineral compositions consistent with forsteritic olivine consistent with a history of differentiation or a composition similar to CK-type meteorites. However, *Masiero et al.* (2014) instead interpret the surface properties as consistent with shock-darkening of silicates (cf. *Britt & Pieters* 1994, *Reddy et al.* 2014). Future work will enable us to resolve the ambiguity in the composition of these objects. The Eos family represents one of the key fronts of advancing our understanding of family formation that has been opened by our wealth of new data.

3.2.8 Themis

The Themis family (PDS ID 602) is one of the largest low-albedo families in the Main Belt. The majority of Themis family members are classified as C-complex bodies (*Mothé-Diniz et al.* 2005; *Ziffer et al.* 2011). Spectral surveys have found variations in the spectral slope among Themis members, ranging from neutral to moderately red (*Ziffer et al.* 2011; *de Leon et al.* 2012). As the first asteroid discovered to show cometary activity (133P Elst-Pizarro) is dynamically associated with Themis, *Hsieh & Jewitt* (2006) searched 150 other Themis family members for signs of cometary activity, discovering one additional object: (118401) 1999 RE₇₀. The periodic nature of this activity points to volatile sublimation as the probable cause, as opposed to collisions or YORP spin up (see the chapter by

Jewitt et al. in this volume) meaning that the Themis family members, and (24) Themis itself, likely harbor subsurface ice. Further, *Rivkin & Emery* (2010) and *Campins et al.* (2010) reported evidence of water ice features on the surface of (24) Themis. If this icy material was primordial to the Themis parent and not implanted by a later impact, this would set constraints on where the Themis parent formed relative to the “snow line” in the protosolar nebula. These objects are also likely to be a new reservoir of water, and may have contributed to the volatile content of the early Earth.

3.2.9 Sylvia

The Sylvia family (PDS ID 603) in the Cybele region, resides at the outer edge of the Main Belt ($3.27 < a \leq 3.70$ AU, *Zellner et al.*, 1985b), beyond the 2:1 Jupiter mean motion resonance. These asteroids, along with the objects in the Hilda and Jupiter Trojan populations, likely have limited contamination by materials from the inner solar system, and represent a pristine view of the materials present near Jupiter at the end of planetary migration. The Nice model proposed that these asteroids are trans-Neptunian objects (TNOs) that were scattered inward during the chaotic phase of planetary evolution (*Levison et al.*, 2009), however the Cybeles show different spectral characteristics from the Hildas and Trojans, and thus may represent the material native to this region of the solar system.

Kasuga et al. (2012) studied the size- and albedo-distributions of the Sylvia asteroid family to better understand the history of these bodies. They found that the largest Cybeles ($D > 80$ km) are predominantly C- or P-types, and the best-fit power law to the size distribution is consistent with a catastrophic collision. However the estimated mass and size of the parent body lead to collisional timescales larger than the age of the solar system, assuming an equilibrium collisional cascade. These are comparable to the timescales for the Hildas, although they find that the Trojan population is consistent with collisional origin. Numerical simulations of the collisional formation and dynamical evolution of the Cybeles will allow for a more detailed study of the history of this population.

3.3 Relationship between albedo and color

Almost every major taxonomic class of asteroid is represented in the list of asteroid families. Using the physical property data described above, we can investigate relationships between the averaged physical properties for each family. By nature of the large sample sizes, the SDSS colors and optical albedos are the best-determined parameters for the majority of families. Figure 2 shows the composite a^* and $i - z$ colors derived for each family from SDSS compared to the composite optical albedo as determined via thermal radiometry. There is a clear linear correlation between the SDSS a^* color and the log of the albedo, although with significant scatter. The $i - z$ color is approximately

flat for low and moderate albedos, but decreases noticeably for high albedo families. It is important to again note that these data are subject to observational selection and completeness biases, and so these relations should be interpreted with caution.

4. DISCUSSION

4.1 Correlation of Observed Properties with the Primordial Composition of the Main Belt

When considering the distributions of colors and albedos, asteroid families fall in one of only a small number of groupings. The Hungaria, Vesta, and Eos families have unique properties that distinguish them from all other families. Similarly, the Watsonia family shows unique polarimetric properties. While the properties of these families can be used to efficiently identify family members and mineral analogs, it is more difficult to relate the mineralogy and history of these families to that of the currently observed Main Belt as a whole (although they may be good analogs for now-extinct populations, cf. *Bottke et al.* 2012).

Conversely, almost all other families fall into either the S-complex or the C-complex, both of which can be further subdivided by spectral taxonomic properties. Given the number of different parent bodies with these compositions, it has been inferred that these two complexes are probes of the pristine material from the protoplanetary disk in this region of the solar system. However, studies of the evolution of the giant planets in the early solar system call into question the specific locations these bodies originated from (e.g. *Gomes et al.* 2005). One possible scenario, known as the “Grand Tack” (*Walsh et al.* 2012), postulates that the protoplanetary core of Jupiter migrated through the planetesimal disk, evacuating the Main Belt region of its primordial material and repopulating it with material from both inward and outward in the disk (see the chapter by *Morbidelli et al.* in this volume). In this case, the two different compositional complexes would represent these implanted objects. Further study of the physical properties of asteroid families and the other small body populations of the solar system will allow us to test this theory.

4.2 Properties of Observed Families Contrasted with the Background Population

Using computed a^* colors from the SDSS MOC 4, *Parker et al.* (2008) divided asteroid families into blue and red groups, tracing the C and S taxonomic complexes, respectively. For both groups, they found that family membership as a fraction of total population increased with decreasing brightness from $\sim 20\%$ at $H_V = 9$ to $\sim 50\%$ at $H_V = 11$. For objects with absolute magnitudes of $H > 11$ the fractions of blue and red asteroids in families diverge, with blue objects in families making up a smaller fraction of

the total population while red objects stay at the levels seen at brighter magnitudes, however it is unclear what contribution the survey biases have to these observed differences. If this difference in behavior is indeed a physical effect, it may indicate a difference in internal structure or collisional processing rates between the two populations.

When exploring the taxonomic distribution of asteroids as a function of distance from the Sun, families have been problematic because the large number of homogeneous objects concentrated in small regions of orbital-element space can skew the results. Studies of the overall distributions of physical properties therefore typically use only the largest member of the family, removing the smaller members (e.g. *Mothe-Diniz et al.* 2003). Alternatively, the distribution could be explored by volume or mass, in which case all family members may be included because their individual volumes or masses contribute to the whole (e.g. *DeMeo & Carry* 2013).

A comprehensive study of the taxonomic contribution of families to the population of small asteroids has not yet been undertaken, however disentangling families from the background is critical to correctly interpreting an overall picture of the compositional make up of the asteroid belt and how the asteroid belt and the bodies within it formed. Distinguishing between families and the background becomes increasingly difficult at smaller sizes where orbital parameters have evolved further due to gravitational and non-gravitational forces. Even the background itself is likely composed of many small families forming from small parent bodies (*Morbidelli et al.* 2003).

4.3 Families as Feeders for the NEO Population

The Yarkovsky and YORP non-gravitational effects play a critical role in repopulating the near-Earth objects with small bodies from the Main Belt (*Bottke et al.* 2000). Primordial asteroids with diameters of ~ 100 m should be efficiently mobilized from their formation locations into a gravitational resonance over the age of the solar system, limiting the contribution of these objects to the currently observed NEO population. However, family formation events act as an important source of objects in this size regime, injecting many thousands of small asteroids into the Main Belt with each impact (*Durda et al.* 2007). The complete census of family physical properties, combined with better estimates for family ages that can now be made, enable us to trace the history of specific near-Earth asteroids from their formation in the Main Belt to their present day orbits. For the same reasons, recently fallen meteorites are also good candidates for comparisons to asteroid families, however the differences between the surface properties we can observe on asteroids and the atmosphere-selected materials surviving to the ground complicate this picture.

4.4 Families Beyond The Main Belt

Although the vast majority of known asteroid families are in the Main Belt, massive collisions resulting in family

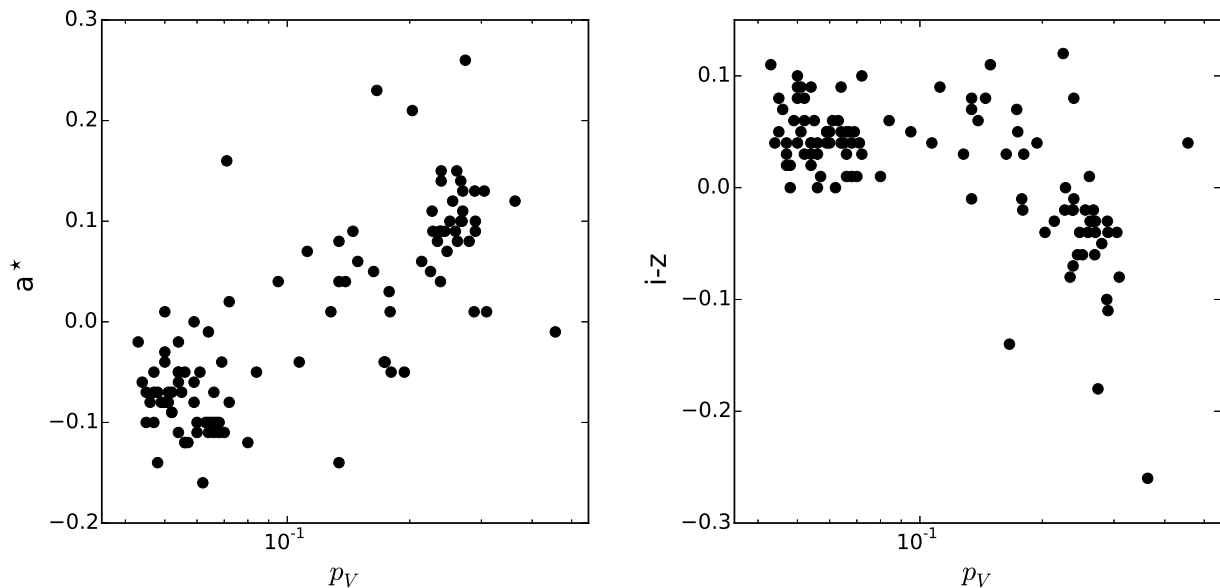


Fig. 2.— Average SDSS a^* and $i - z$ colors compared with optical albedos for asteroid families, as given in Table 1

formation events are not unique to this region of the solar system. While the near-Earth asteroid population is dynamically young (*Gladman et al. 2000*) and thus these objects have a low probability of undergoing collisional breakup, the more distant reservoirs that date back to the beginning of the solar system are expected to undergo the same collisional processing as the Main Belt, albeit with lower impact velocities. Searches for young families in both the NEO and Mars Trojan populations have yielded only a single candidate family cluster associated with (5261) Eureka (*Schunová et al. 2012; Christou 2013*). Dynamical families have been identified in the Hilda, Jupiter Trojan, and TNO populations. The first two populations are trapped in long-term stable resonant orbits with Jupiter, providing a population that has suffered far less dispersion than the majority of Main Belt families. Similarly, the TNO population is cross-cut by a range of Neptune resonances, some of which are similarly long-term stable. The Yarkovsky and YORP effects are greatly diminished for all three populations compared to the Main Belt (especially the TNOs) due to the larger distances to the Sun, further reducing the dispersion of collisional fragments.

Grav et al. (2012) present visible and infrared albedos for the Hilda and Schubart asteroid families found in the 3:2 Jupiter mean motion resonance. Using these albedos, they show the Hilda family is associated with D-type taxonomy, while the Schubart family is associated with C or P-type taxonomy. The Hilda population in general is dominated by C and P-type objects at the largest sizes measured, but transitions to primarily D-class at the smallest sizes measured, which may be indicative of the effect of the Hilda family on the overall population (*Grav et al. 2012; DeMeo & Carry, 2014*). However we note that recent family analysis by *Mi-*

lani et al. (2014) showed that the Hilda family was not statistically significant using their methodology, in contrast to previous work.

The Jupiter Trojans are comprised of the L4 and L5 Lagrange point swarms which lead and trail Jupiter (respectively) on its orbit. Multiple families have been identified in each of the swarms (*Milani 1993, Beaugé & Roig, 2001*), however there is some debate as to the significance of these families (cf. *Brož & Rozehnal, 2011*). *Fornasier et al. (2007)* combined measured spectra from multiple sources (*Fornasier et al. 2004, Dotto et al. 2006*) to characterize Trojan family members. In the L5 cloud, members of the Aeneas, Anchises, Misenus, Phereclos, Sarpedon, and Panthoos families were found to have spectra with moderate-to-high spectral slopes, with most members being classified as D-type. The background population had a wider range of slopes and taxonomies from P- to D-type (*Fornasier et al., 2004*).

In the L4 cloud members of the Eurybates, 1986 WD and 1986 TS₆ families were studied. The 1986 WD and 1986 TS₆ family members had featureless spectra and high slopes resulting in a classification for most as D-types, while the few with lower slopes were placed in the C- and P-classes. Eurybates members, however, have markedly different spectra with low to moderate slopes splitting the classifications evenly between the C- or P-classes (*Fornasier et al. 2007, DeLuise et al. 2010*). *Roig et al. (2008b)* used the SDSS data to investigate asteroid families in the Jupiter Trojan population, and found that the families in the Trojan populations account for the differences in the compositional distributions between the L4 and L5 clouds. In particular, the families in the L4 cloud show an abundance of C- and P-type objects not reflected in the L5 families or the back-

ground populations in either cloud.

The TNO population covers a much larger volume of space than any of the populations of objects closer to the Sun, but is also estimated to contain over 1000 times the mass of the Main Belt. Collisions resulting in catastrophic disruptions are believed to have occurred at least twice in the TNO population. Pluto's five (or potentially more; *Weaver et al.* 2006) satellites speak to a massive collision, which will be a key area of investigation of the New Horizons flyby of the Pluto system.

The dwarf planet Haumea is highly elongated with a very short rotational period (~ 4 hours), is orbited by two small satellites, has a relatively high density, and has a spectrum that is consistent with nearly pure water ice. These properties are thought to be the result of a mantle-shattering collisional event, though the details of this event remain contentious. A group of TNOs with colors substantially bluer than the typical neutral-to-ultra-red surfaces of the Kuiper Belt, all sharing high inclinations similar to Haumea, has been identified as a collisional family produced by this event (*Brown et al.* 2007). Because of the orbital velocity regimes in trans-Neptunian space, collisional families are in general unlikely to be identified there through dynamics alone (as they are in the asteroid belt). It was only through the unique composition of the family members (akin to the extremely distinct photometric properties of the Vesta family members) that the Haumea family could be readily identified. This implies that more collisional families may be hiding in the TNO population, but cannot be spotted by orbits alone.

Although massive collisions dominated the solar system environment during the epoch of planet building, they also played an important role in shaping all of the major populations of small bodies during the subsequent ~ 4 billion years. Collisional evolution, although stochastic in nature, was a major determinant in the structure of the solar system we see today (see the chapter by *Bottke et al.* in this volume).

5. OPEN PROBLEMS AND FUTURE PROSPECTS

The effect of space weathering on asteroidal surfaces still remains an important topic for future exploration (see the chapter by *Brunetto et al.* in this volume for further discussion). The range of studies carried out so far have found a wide dispersion of results, both in terms of the timescale of weathering and the specific effects on various taxonomic classes. Studies to date have relied on the assumption that all asteroids with similar taxonomic types have identical mineralogical compositions, or have been based on a single pair of families known to be compositionally identical but with different ages (i.e. Karin and Koronis). As deeper surveys and dynamical analysis techniques begin to increase the number of identified cases of family-within-a-family, physical studies of these interesting populations will allow

better measurements of the specific effects and timing of space weathering processes.

Advances in physical measurements of asteroid families have not uniformly addressed the various parameters needed for a robust scientific investigation. In particular, there has been only a nominal advancement in the measurement of asteroid masses and densities, owing to the difficulty in determining these parameters. *Carry* (2012) compiled known measurements of asteroid densities into a comprehensive list, however only a handful of families have more than one member represented, and for most the only measurement is of the largest remnant body. A larger survey of densities including many family members over a range of sizes would enable testing of family formation conditions via reaccretion (cf. chapter by *Michel et al.* in this volume), as well as improve family ages derived from numerical simulations of gravitational and Yarkovsky orbital evolution (cf. chapter by *Nesvorný et al.* in this volume). This could be accomplished by a more comprehensive search for binaries, or through modeling of gravitational perturbations to asteroid orbits detectable in next-generation astrometric catalogs.

One highly-anticipated survey will be carried out by the European Space Agency's Gaia mission (*Hestroffer et al.*, 2010), which is expected to provide spectral characterization of all objects down to an apparent magnitude of $V = 20$, including many asteroid family members (*Campins et al.* 2012; *Delbo et al.* 2012; *Cellino & Dell'Oro*, 2012). This dramatic increase in the number of characterized family members will enable a host of new investigations of the composition and differentiation of family parent bodies. By spectrally probing bodies as small as ~ 2 km, inhomogeneities in asteroid family composition may begin to be revealed. Another key scientific product will be refined astrometry for all asteroids which can be searched for gravitational perturbations and used to determine the masses of the largest asteroids (*Mignard et al.*, 2007). This wealth of new data will feed into theoretical models and numerical simulations, allowing us to improve the ages determined from orbital evolution simulations (e.g. *Masiero et al.*, 2012; *Caruba et al.*, 2014).

The collision events that form families are very rare, and the probability of a massive collision in the next ten, hundred, or thousand years is vanishingly small (see chapter by *Bottke et al.* in this volume). However, a new class of active Main Belt objects has recently been identified that may none-the-less provide a window into the collisional environment of the solar system (see the chapter by *Jewitt et al.* in this volume for further discussion). While some of these objects show repeated activity indicative of a cometary nature complete with sub-surface volatiles, others are best explained by impact events. In particular, the observed outburst events of P/2010 A2 (*Jewitt et al.* 2010) and (596) Scheila (*Jewitt et al.* 2011) are consistent with impacts by very small ($D < 50$ m) asteroids. As current and future sky surveys probe to smaller diameters in the Main Belt, the frequency these events will be observed, or even predicted

in advance, will increase. Study of these small scale disruptions offers an important constraint on impact physics in the low-gravity environment of asteroids, and provides test cases for comparing to the small-scale impact experiments that can be performed in Earth-based laboratories.

Recently, *Reddy et al.* (2014) presented evidence that shock darkening may play a role in altering the spectroscopic properties of chondritic materials in the Baptistina and Flora families. If evidence for this effect is seen in other families across a range of compositions, this technique may provide a method for determining the conditions of family-forming impacts in the Main Belt, and thus provide better constraints on the ages of families. This may also help explain some of the differences observed in space weathering studies that find albedo changes happen very quickly while spectral changes have long timescales.

As new data sets have rapidly increased our ability to characterize asteroid family members, and through this the parent body from which they originated, one glaring question remains at the forefront of the field: where are the families of differentiated parent bodies that were completely disrupted? Vesta and its family members have given us a excellent example of the composition and resultant albedo, color, and spectral properties of the crust of a differentiated body (see the chapter by *Russell et al.* in this volume for further discussion). However, searches for objects with similar properties in different regions of the Main Belt have yielded no significant populations of these basaltic crust and mantle fragments that should be leftover from these collisions. On the other hand, data from iron meteorites has indicated that differentiation of protoplanets, if not common, at a minimum happened multiple times (see chapters by *Elkins-Tanton et al.* and *Scott et al.* in this volume for further discussion). While it is possible that these collisions happened at the earliest stages of the solar system's formation and the evidence (in the form of families) was erased during the epoch of giant planet migration that is the foundation of the 'Nice' model (see chapter by *Morbidelli et al.* in this volume), a dynamical explanation of this problem would need to preserve in the Main Belt the core material that still falls to Earth today. Conversely, if these impacts happened after the last great shake up of the solar system, a mineralogical explanation for how metallic cores could form without leaving a basaltic 'residue' in the Main Belt is required. The limitations on what *could not* have happened that are being set by current surveys are just as important as our discoveries of what did happen.

The next decade of large surveys, both ground- and space-based, promises to expand our knowledge of asteroid physical properties by potentially another order of magnitude beyond what is known today. In this data-rich environment, family research will focus not just on individual families and their place in the Main Belt, but on specific sub-groupings within families: on the knots, clumps, and collisional cascade fragments that trace the disruption and evolutionary dynamics that families have undergone. As the sizes of objects probed reach smaller and smaller, we

can expect to find more young families like Karin and Ianini that can be directly backward-integrated to a specific time of collision, improving our statistics of collisions in the last 10 million years. As catalogs increase in size, we can also expect to more frequently have characterization data of objects both before and after they undergo catastrophic disruption. This will enable us to test our impact physics models on scales not achievable on Earth. Additionally, we will begin to see a time when we routinely use remote sensing data of asteroids to not just associate families but assess the mineralogy of family members as a probe of the parent body. Asteroid family physical properties, numerical simulations, and evolutionary theory will leapfrog off of each other, pushing forward our understanding of the asteroids and of the whole solar system.

Acknowledgments. JRM was partially supported by a grant from the NASA Planetary Geology and Geophysics Program. FED was supported by NASA through the Hubble Fellowship grant HST-HF-51319.01-A, awarded by the Space Telescope Science Institute, which is operated by the Association of Universities for Research in Astronomy, Inc., for NASA, under contract NAS 5-26555. This publication makes use of data products from the Wide-field Infrared Survey Explorer, which is a joint project of the University of California, Los Angeles, and the Jet Propulsion Laboratory/California Institute of Technology, funded by the National Aeronautics and Space Administration. This publication also makes use of data products from NEO-WISE, which is a project of the Jet Propulsion Laboratory/California Institute of Technology, funded by the Planetary Science Division of the National Aeronautics and Space Administration. Funding for the creation and distribution of the SDSS Archive has been provided by the Alfred P. Sloan Foundation, the Participating Institutions, the National Aeronautics and Space Administration, the National Science Foundation, the U.S. Department of Energy, the Japanese Monbukagakusho, and the Max Planck Society. The SDSS Web site is <http://www.sdss.org/>. The SDSS is managed by the Astrophysical Research Consortium (ARC) for the Participating Institutions. The Participating Institutions are The University of Chicago, Fermilab, the Institute for Advanced Study, the Japan Participation Group, The Johns Hopkins University, the Korean Scientist Group, Los Alamos National Laboratory, the Max-Planck-Institute for Astronomy (MPIA), the Max-Planck-Institute for Astrophysics (MPA), New Mexico State University, University of Pittsburgh, University of Portsmouth, Princeton University, the United States Naval Observatory, and the University of Washington. This research is based on observations with AKARI, a JAXA project with the participation of ESA. The authors wish to thank Bobby Bus, Beth Ellen Clark, Heather Kaluna, and Pierre Vernazza for providing proprietary spectra to include in Figure 1. We also thank the referees, Alberto Cellino and Bobby Bus, and editor Patrick Michel for helpful comments that improved this chapter.

TABLE 1
PHYSICAL PROPERTIES OF ASTEROID FAMILIES

Number	Name	PDS ID	$\langle P_V \rangle$	n_{PV}	$\langle PNIR \rangle$	n_{PNIR}	$\langle a^* \rangle$	$\langle i - z \rangle$	n_{SDSS}	SFD slope	SFD range (km)	Tax	n_{tax}
2	Pallas	801	0.134+/-0.026	49	0.114+/-0.047	10	-0.14+/-0.03	-0.01+/-0.08	13	.../-...	...	B	8
3	Juno	501	0.262+/-0.054	125	0.488+/-0.000	8	0.08+/-0.05	-0.03+/-0.07	87	-2.427+/-0.108	2.7-7.3	Sq	1
4	Vesta	401	0.363+/-0.088	1900	0.465+/-0.156	54	0.12+/-0.05	-0.26+/-0.10	2148	-3.417+/-0.030	2.5-11.9	V	49
8	Flora	402	0.305+/-0.064	1330	0.440+/-0.082	142	0.13+/-0.06	-0.04+/-0.07	922	-2.692+/-0.030	2.8-12.2	S	74
10	Hygiea	601	0.070+/-0.018	1951	0.065+/-0.028	3	-0.11+/-0.05	0.01+/-0.07	606	-3.883+/-0.040	6.1-19.3	C	1
15	Eunomia	502	0.270+/-0.059	1448	0.374+/-0.088	148	0.13+/-0.05	-0.03+/-0.06	798	-3.091+/-0.033	4.4-17.6	S	30
20	Massalia	404	0.247+/-0.053	214	...	0	0.07+/-0.05	-0.04+/-0.08	386	-3.544+/-0.140	2.0-4.1	S	1
24	Themis	602	0.068+/-0.017	2218	0.07+/-0.030	86	-0.11+/-0.04	0.01+/-0.06	640	-2.313+/-0.017	7.3-55.6	S	39
25	Phocaea	701	0.290+/-0.066	715	0.355+/-0.203	119	0.10+/-0.11	-0.04+/-0.08	252	-2.663+/-0.039	3.5-14.6	S	1
27	Euterpe	410	0.270+/-0.062	45	0.493+/-0.000	1	0.11+/-0.05	-0.04+/-0.08	42	S	1
31	Euphrosyne	901	0.059+/-0.013	742	0.082+/-0.173	5	-0.08+/-0.05	0.04+/-0.06	169	-4.687+/-0.082	7.3-18.4	Cb	1
44	Nysa(Polana)	405	0.289+/-0.074	1345	0.356+/-0.059	22	0.13+/-0.06	-0.03+/-0.07	1544	-3.083+/-0.030	2.5-13.0	...	0
46	Hestia	523	0.267+/-0.049	28	0.068+/-0.000	1	-0.04+/-0.04	-0.03+/-0.04	22	Xc	1
81	Terpsichore	413	0.059+/-0.010	57	0.053+/-0.000	1	-0.08+/-0.03	0.08+/-0.10	15	-4.371+/-0.508	5.0-7.3	Cb	1
84	Klio	603	0.059+/-0.014	107	0.089+/-0.031	3	-0.06+/-0.04	0.05+/-0.08	23	-2.478+/-0.129	3.3-8.0	Ch	1
87	Sylvia	603	0.051+/-0.012	121	0.082+/-0.000	1	-0.07+/-0.05	0.09+/-0.11	20	-3.339+/-0.232	7.0-12.4	X	1
89	Julia	540	0.225+/-0.036	2	0.339+/-0.000	2	0.05+/-0.02	0.12+/-0.07	3	Ld	1
96	Aegle	630	0.072+/-0.013	83	0.102+/-0.000	1	0.02+/-0.05	0.10+/-0.08	23	-3.252+/-0.305	6.8-11.4	T	1
128	Nemesis	504	0.072+/-0.019	347	0.071+/-0.000	1	-0.08+/-0.06	0.03+/-0.07	109	-4.320+/-0.121	3.8-8.4	C	2
137	Meliboea	604	0.060+/-0.013	163	0.050+/-0.029	12	-0.10+/-0.08	0.05+/-0.07	53	-1.513+/-0.051	8.0-39.4	Ch	11
142	Polana(Nysa)	n/a	0.056+/-0.012	1130	0.061+/-0.006	3	-0.12+/-0.10	0.00+/-0.08	375	-3.177+/-0.041	3.6-12.4	B	3
144	Vibilia	529	0.065+/-0.011	180	...	0	-0.10+/-0.04	0.04+/-0.07	35	-3.137+/-0.135	4.5-9.7	Ch	1
145	Aedona	505	0.060+/-0.011	874	0.068+/-0.078	19	-0.11+/-0.08	0.04+/-0.07	274	-2.854+/-0.037	5.3-23.2	Ch	12
148	Gallia	802	0.251+/-0.059	24	...	0	0.10+/-0.03	-0.06+/-0.06	15	Sl	1
158	Koronis	605	0.238+/-0.051	1089	0.325+/-0.059	67	0.09+/-0.07	-0.02+/-0.08	810	-2.451+/-0.026	5.1-32.0	S	34
163	Erigone	406	0.051+/-0.010	716	0.061+/-0.013	17	-0.08+/-0.10	0.05+/-0.08	201	-3.215+/-0.050	3.3-11.9	Ch	1
170	Maria	506	0.255+/-0.061	1361	0.370+/-0.068	69	0.12+/-0.05	-0.02+/-0.07	809	-2.637+/-0.025	3.5-24.8	S	23
173	Ino	522	0.244+/-0.069	90	...	0	0.09+/-0.05	-0.06+/-0.07	93	-3.141+/-0.268	2.7-4.6	...	0
221	Eos	606	0.163+/-0.035	3509	0.180+/-0.053	205	0.05+/-0.05	0.03+/-0.07	1692	-2.222+/-0.013	5.6-47.3	K	30
283	Emma	607	0.047+/-0.011	260	0.118+/-0.113	2	-0.07+/-0.06	0.04+/-0.08	75	-3.442+/-0.113	6.7-15.3	C	1
293	Brasilia	608	0.174+/-0.048	110	0.224+/-0.017	4	-0.04+/-0.04	0.05+/-0.07	78	-3.462+/-0.243	3.7-6.4	X	2
298	Baptistina	403	0.179+/-0.056	581	0.390+/-0.198	25	0.01+/-0.09	-0.02+/-0.09	321	-3.254+/-0.063	2.5-7.2	S	9
302	Claritha	407	0.048+/-0.010	44	...	0	-0.14+/-0.04	0.00+/-0.06	10	F	1
313	Chaldaeia	415	0.063+/-0.017	169	0.083+/-0.039	11	-0.10+/-0.05	0.06+/-0.07	34	-3.058+/-0.119	3.7-8.6	C	3
322	Phaeo	530	0.059+/-0.015	99	0.181+/-0.000	2	0.00+/-0.06	0.05+/-0.08	34	-2.852+/-0.195	5.1-10.1	D	1
329	Svea	416	0.050+/-0.009	30	0.134+/-0.166	2	-0.04+/-0.06	0.04+/-0.05	8	C	1
363	Padua	507	0.069+/-0.015	427	0.067+/-0.022	5	-0.04+/-0.06	0.05+/-0.07	135	-2.588+/-0.053	4.5-16.4	X	10
369	Aeria	539	0.180+/-0.011	22	0.266+/-0.000	6	-0.05+/-0.04	0.03+/-0.09	18	M	1
375	Ursula	631	0.061+/-0.014	600	0.083+/-0.047	15	-0.05+/-0.08	0.06+/-0.09	194	-2.677+/-0.046	7.3-27.2	...	0
396	Aeolia	508	0.107+/-0.022	43	0.115+/-0.000	1	-0.04+/-0.05	0.04+/-0.03	10	Xe	1
410	Chloris	509	0.084+/-0.031	171	0.081+/-0.095	10	-0.05+/-0.08	0.06+/-0.05	59	-2.814+/-0.103	5.2-14.0	C	8
434	Hungaria	003	0.456+/-0.217	527	0.727+/-1.692	9	-0.01+/-0.08	0.04+/-0.10	636	Xe	14
480	Hansa	803	0.269+/-0.067	316	0.377+/-0.068	9	0.10+/-0.05	-0.06+/-0.07	134	-3.378+/-0.104	3.4-7.9	S	2
490	Veritas	609	0.066+/-0.016	697	0.068+/-0.011	3	-0.07+/-0.04	0.05+/-0.08	207	-2.744+/-0.043	5.8-22.6	Ch	8
495	Eulalia(Polana)	n/a	0.057+/-0.012	2008	0.066+/-0.029	15	-0.12+/-0.05	0.01+/-0.07	531	-2.687+/-0.021	3.0-18.4	C	13
569	Misa	510	0.052+/-0.013	287	0.064+/-0.027	3	-0.07+/-0.07	0.03+/-0.08	79	-2.508+/-0.067	4.0-13.3	Ch	1
589	Croatia	638	0.054+/-0.010	99	0.068+/-0.000	1	-0.05+/-0.04	0.02+/-0.09	22	-3.383+/-0.224	5.8-11.1	X	1
606	Brangane	511	0.112+/-0.028	44	0.137+/-0.000	2	0.07+/-0.04	0.09+/-0.06	20	L	1
618	Elfriede	632	0.052+/-0.012	36	0.063+/-0.000	1	-0.09+/-0.05	0.06+/-0.05	8	C	1
623	Chimaera	414	0.054+/-0.012	63	0.049+/-0.000	3	-0.05+/-0.03	0.09+/-0.10	20	-2.586+/-0.235	3.8-7.2	XC	1
627	Charis	616	0.071+/-0.010	39	0.264+/-0.000	2	0.16+/-0.06	0.04+/-0.08	59	X	1
656	Beagle	620	0.080+/-0.014	30	0.070+/-0.006	5	-0.12+/-0.03	0.01+/-0.06	16	X	1
668	Dora	512	0.056+/-0.012	667	0.047+/-0.017	17	-0.12+/-0.07	0.04+/-0.07	175	-2.610+/-0.043	5.7-21.6	Ch	29
686	Gersuind	804	0.145+/-0.037	106	0.328+/-0.000	1	0.09+/-0.07	0.08+/-0.07	36	-2.653+/-0.158	3.8-8.0	...	0
702	Alauda	902	0.066+/-0.015	687	0.071+/-0.013	26	-0.10+/-0.06	0.03+/-0.07	197	-2.707+/-0.042	9.2-36.7	...	0
709	Fringilla	623	0.050+/-0.014	51	0.212+/-0.788	2	-0.03+/-0.06	0.09+/-0.08	24	X	1
729	Watsonia	537	0.134+/-0.019	51	0.181+/-0.000	2	0.08+/-0.04	0.07+/-0.02	12	L	2
752	Salamitis	408	0.055+/-0.011	134	0.048+/-0.000	1	-0.07+/-0.07	0.06+/-0.11	33	-2.417+/-0.126	3.8-8.8	Ch	1
778	Theobalda	617	0.062+/-0.016	107	0.070+/-0.000	1	-0.16+/-0.03	0.00+/-0.05	28	-3.097+/-0.185	6.5-13.3	...	0
780	Armenia	905	0.056+/-0.013	28	0.060+/-0.000	2	-0.05+/-0.01	0.03+/-0.04	4	C	1
808	Merxia	513	0.234+/-0.054	93	0.347+/-0.030	3	0.08+/-0.05	-0.08+/-0.08	98	-2.662+/-0.190	3.2-6.7	S	6
832	Karin	610	0.178+/-0.031	18	0.294+/-0.000	1	0.03+/-0.05	-0.01+/-0.07	33	S	47
845	Naema	611	0.064+/-0.012	155	0.055+/-0.000	1	-0.10+/-0.11	0.04+/-0.06	45	-4.274+/-0.220	6.0-10.6	C	1
847	Agnia	514	0.238+/-0.060	110	0.389+/-0.015	3	0.04+/-0.05	-0.07+/-0.08	179	-3.055+/-0.165	3.8-8.0	S	8
909	Ulla	903	0.048+/-0.009	19	...	0	-0.07+/-0.02	0.02+/-0.06	3	X	1
918	Itha	633	0.239+/-0.056	28	0.353+/-0.084	8	0.14+/-0.04	-0.01+/-0.05	14	Sl	4
945	Barcelona	805	0.290+/-0.064	52	0.510+/-0.000	1	0.09+/-0.05	-0.11+/-0.09	21	Sq	1
1128	Astrid	515	0.045+/-0.010	213	0.046+/-0.000	1	-0.07+/-0.05	0.08+/-0.08	33	-2.567+/-0.080	3.5-11.1	C	5
1189	Terentia	618	0.064+/-0.012	13	0.058+/-0.000	1	-0.01+/-0.00	0.09+/-0.00	1	Ch	1
1222	Tina	806	0.128+/-0.042	26	0.137+/-0.000	1	0.01+/-0.00	0.03+/-0.05	3	X	1
1270	Datura	411	0.288+/-0.000	1	...	0	0.01+/-0.00	-0.10+/-0.00	1	S	4
1272	Gefion	516	0.267+/-0.058	737	0.350+/-0.154	25	0.10+/-0.06	-0.02+/-0.07	523	-3.262+/-0.050	4.0-14.3	S	32
1303	Luthera	904	0.050+/-0.009	125	0.078+/-0.000	1	0.01+/-0.04	0.10+/-0.07	39	-3.955+/-0.264	7.9-13.0	...	0
1332	Marconia	636	0.042+/-0.008	6	0.080+/-0.000	1	0	L	1
1400	Tirela	612	0.239+/-0.057	419	0.073+/-0.095	7	0.15+/-0.09	0.08+/-0.08	225	-3.454+/-0.073	4.8-14.3	Ld	10
1484	Postrema	541	0.047+/-0.010	30	0.051+/-0.006	3	-0.05+/-0.05	0.02+/-0.06	5	B	1
1658	Innes	518	0.259+/-0.057	195	0.318+/-0.149	8	0.09+/-0.06	-0.04+/-0.07	163	-3.385+/-0.128	3.1-7.0	S	2
1668	Hanna	533	0.052+/-0.011	102	0.048+/-0.000	1	-0.09+/-0.03	0.08+/-0.05	20	-3.502+/-0.240	3.9-7.2	...	0
1726	Hoffmeister	519	0.047+/-0.010	609	0.052+/-0.013	4	-0.10+/-0.05	0.03+/-0.08	145	-2.856+/-0.047	4.5-17.2	C	9
1892	Lucienne	409	0.228+/-0.029	19	...	0	0.09+/-0.03	0.00+/-0.09	10	S	1
2085	Henan	542	0.227+/-0.065	106	0.165+/-0.000	3	0.11+/-0.06	-0.02+/-0.09	163	-3.667+/-0.276	3.4-5.8	L	1
2262	Mitidika	531	0.066+/-0.014	279	0.060+/-0.013	10	-0.11+/-0.06	0.01+/-0.08	71	-2.832+/-0.091	4.6-11.4	...	0
2344	Xizang	536	0.134+/-0.044	18	...	0	0.04+/-0.05	0.08+/-0.07	12	0
238													

TABLE 1—*Continued*

Number	Name	PDS ID	$\langle p_V \rangle$	n_{p_V}	$\langle p_{NIR} \rangle$	$n_{p_{NIR}}$	$\langle a^* \rangle$	$\langle i - z \rangle$	n_{SDSS}	SFD slope	SFD range (km)	Tax	n_{tax}
7353	Kazuia	532	0.214 \pm 0.025	13	... \pm ...	0	0.06 \pm 0.08	-0.03 \pm 0.02	3	... \pm	L	1
7468	Anfimov	635	0.166 \pm 0.061	10	... \pm ...	0	0.23 \pm 0.03	-0.14 \pm 0.09	13	... \pm	0
7481	SanMarcello	626	0.194 \pm 0.054	27	... \pm ...	0	-0.05 \pm 0.04	0.04 \pm 0.06	18	... \pm	0
9506	Telramund	614	0.237 \pm 0.063	46	... \pm ...	0	0.09 \pm 0.05	-0.02 \pm 0.09	33	... \pm	0
10811	Lau	619	0.274 \pm 0.000	1	... \pm ...	0	0.26 \pm 0.00	-0.18 \pm 0.00	1	... \pm	0
14627	Emilkowalski	523	0.149 \pm 0.046	4	... \pm ...	0	0.06 \pm 0.00	0.11 \pm 0.00	1	... \pm	0
15454	1998YB3	627	0.054 \pm 0.006	11	... \pm ...	0	-0.11 \pm 0.03	0.04 \pm 0.03	7	... \pm	0
15477	1999CG1	628	0.095 \pm 0.030	68	... \pm ...	0	0.04 \pm 0.04	0.05 \pm 0.06	25	-4.768 \pm 0.602	4.3-6.0	...	0
16598	1992YC2	524	... \pm ...	0	... \pm ...	0	0.10 \pm 0.00	-0.09 \pm 0.00	1	... \pm	Sq	1
18405	1993FY12	615	0.173 \pm 0.049	15	... \pm ...	0	-0.04 \pm 0.03	0.07 \pm 0.08	12	... \pm	0
36256	1999XT17	629	0.203 \pm 0.066	13	... \pm ...	0	0.21 \pm 0.07	-0.04 \pm 0.05	6	... \pm	0
53546	2000BY6	526	0.139 \pm 0.000	1	... \pm ...	0	0.04 \pm 0.03	0.06 \pm 0.04	9	... \pm	0
106302	2000UJ87	637	0.045 \pm 0.004	12	... \pm ...	0	-0.10 \pm 0.04	0.05 \pm 0.04	3	... \pm	0

REFERENCES

- Alí-Lagoa, V., de León, J., Licandro, et al. (2013) Physical properties of B-type asteroids from WISE data. *Astron. Astrophys.*, 554, A71.
- Assandri, M. C. & Gil-Hutton, R. (2008) Surface composition of Hungaria asteroids from the analysis of the Sloan Digital Sky Survey. *Astron. & Astrophys.*, 488, 339.
- Beaugé, C. & Roig, F. (2001) A Semianalytical Model for the Motion of the Trojan Asteroids: Proper Elements and Families. *Icarus*, 153, 391.
- Bell, J. F. (1988) A probable asteroidal parent body for the CO or CV chondrites. *Meteoritics*, 23, 256.
- Binzel, R. P. & Xu, S. (1993) Chips off of asteroid 4 Vesta - Evidence for the parent body of basaltic achondrite meteorites. *Science*, 260, 186.
- Bottke, W. F., Vokrouhlický, D., Minton, D., et al. (2012) An Archaean heavy bombardment from a destabilized extension of the asteroid belt. *Nature*, 485, 78.
- Bottke, W. F., Vokrouhlický, D., Nesvorný, D., (2007) An asteroid breakup 160Myr ago as the probable source of the K/T impactor. *Nature*, 449, 48.
- Bottke, W. F., Rubincam, D. P. & Burns, J. A. (2000) Dynamical Evolution of Main Belt Meteoroids: Numerical Simulations Incorporating Planetary Perturbations and Yarkovsky Thermal Forces. *Icarus*, 145, 301.
- Bowell, E., Oszkiewicz, D. A., Wasserman, L. H., Muinonen, K., Pentiä, A., Trilling, D. E. (2014) Asteroid spin-axis longitudes from the Lowell Observatory database. *Meteor. & Plan. Sci.*, 49, 95.
- Britt, D. T. & Pieters, C. M., (1991) Black ordinary chondrites: an analysis of abundance and fall frequency. *Meteoritics*, 26, 279.
- Britt, D. T. & Pieters, C. M., (1994) Darkening in black and gas-rich ordinary chondrites: The spectral effect of opaque morphology and distribution *Geochem. et Cosmoch. Acta*, 58, 3905.
- Brown, M. E., Barkume, K. M., Ragozzine, D., Schaller, E. L., (2007) A collisional family of icy objects in the Kuiper belt. *Nature*, 446, 294.
- Brož, M., Morbidelli, A., Bottke, W. F., Rozehnal, J., Vokrouhlický, D., Nesvorný, D., (2013) Constraining the cometary flux through the asteroid belt during the late heavy bombardment. *Astron. & Astrophys.*, 551, A117
- Brož, & M., Morbidelli, A., (2013) The Eos Family Halo *Icarus*, 223, 844.
- Brož, & M., Rozehnal, J., (2011) Eurybates - the only asteroid family among Trojans? *Month. Not. Royal. Astron. Soc.*, 414, 565.
- Burbine, T. H., Gaffey, M. J. & Bell, J. F., (1992) S-asteroids 387 Aquitania and 980 Anacostia - Possible fragments of the breakup of a spinel-bearing parent body with CO3/CV3 affinities. *Meteoritics*, 27, 424.
- Burbine, T. & Binzel, R. P. (2002) Small Main-Belt Asteroid Spectroscopic Survey in the Near-Infrared. *Icarus*, 159, 468.
- Bus, S.J. & Binzel, R.P. (2002) Phase II of the Small Main-Belt Asteroid Spectroscopic Survey: A Feature-Based Taxonomy *Icarus*, 158, 146.
- Campins, H., Hargrove, K., Pinilla-Alonso, N., et al. (2010) Water ice and organics on the surface of the asteroid 24 Themis. *Nature*, 464, 1320.
- Campins, H., de León, J., Licandro, J., et al. (2012) Spectra of asteroid families in support of Gaia. *Planetary and Space Sci.*, 73, 95-97.
- Carruba, V., Michtchenko, T. A., Roig, F., Ferraz-Mello, S. & Nesvorný, D. (2005) On the V-type asteroids outside the Vesta family. I. Interplay of nonlinear secular resonances and the Yarkovsky effect: the cases of 956 Elisa and 809 Lundia. *Astron. & Astroph.*, 441, 819.
- Carruba, V. (2013) An analysis of the Hygiea asteroid family orbital region. *Mon. Not. Roy. Astr. Soc.*, 431, 3557-3569.
- Carruba, V., Domingos, R. C., Nesvorný, D., Roig, F., Huaman, M. E., and Souami, D. (2013) A multidomain approach to asteroid families' identification. *Mon. Not. Roy. Astr. Soc.*, 433, 2075-2096.
- Carruba, V., Aljbaae, S., & Souami, D. (2014) Peculiar Euphrosyne. *Astrop. J.*, 792, 46.
- Carry, B. (2012) Density of asteroids. *Planetary & Space Sci.*, 73, 98.
- Carvano, J. M., Lazzaro, D., Mothé-Diniz, T., Angeli, C. A. & Florczak, M. (2001) Spectroscopic Survey of the Hungaria and Phocaea Dynamical Groups. *Icarus*, 149, 173.
- Carvano, J. M., Hasselmann, P. H., Lazzaro, D., Mothé-Diniz, T. (2010) SDSS-based taxonomic classification and orbital distribution of Main Belt asteroids. *Astron. & Astrophys.*, 510, A43.
- Clark, B. E., Ockert-Bell, M. E., Cloutis, E. A., Nesvorný, D., Mothé-Diniz, T., & Bus, S.J. (2009) Spectroscopy of K-complex asteroids: Parent bodies of carbonaceous meteorites? *Icarus*, 202, 119.
- Cellino, A. & Dell'Oro, A. (2012) The derivation of asteroid physical properties from Gaia observations *Plan & Space Sci.*, 73, 52.
- Cellino A., Gil-Hutton, R., Tedesco, E.F., Di Martino, M. and Brunini, A. (1999) Polarimetric observations of small observations: preliminary results. *Icarus*, 138, 129.
- Cellino, A., Zappala, V., Doressoundiram, A. et al. (2001) The Puzzling Case of the Nysa-Polana Family. *Icarus*, 152, 225.
- Cellino, A., Bus, S.J., Doressoundiram, A. & Lazzaro, D (2002) Spectroscopic properties of asteroid families. *Asteroids III*, 633
- Cellino, A., Delbò, M., Bendjoya, Ph., Tedesco, E. F. (2010) Polarimetric evidence of close similarity between members of the Karin and Koronis dynamical families. *Icarus*, 209, 556.
- Cellino, A., Dell'Oro, A., Tedesco, E.F. (2009) Asteroid Families: Current Situation. *Plan. and Space Sci.*, 57, 173.
- Cellino, A., Bagnulo, S., Tanga, P., Novaković, B., and Delbò, M. (2014) A successful search for hidden Barbarians in the Watsonia asteroid family. *Mon. Not. Roy. Astr. Soc.*, 439, L75-L79.
- Christou, A. A. (2013) Orbital clustering of martian Trojans: An asteroid family in the inner Solar system? *Icarus*, 224, 144.
- Consolmagno, G. J. & Drake, M. J. (1977) Composition and evolution of the eucrite parent body - Evidence from rare earth elements *Geochem. et Cosmochim. Acta*, 41, 1271.
- Delbò, M., Gayon-Markt, J., Busso, G., et al. (2012) Asteroid spectroscopy with Gaia. *Plan. & Space Sci.*, 73, 86.
- de Leon, J., Licandro, J., Serra-Ricart, M., Pinilla-Alonso, N. & Campins, H (2010) Observations, compositional, and physical characterization of near-Earth and Mars-crosser asteroids from a spectroscopic survey. *Astorn. & Astroph.*, 517, 23.
- de León, J., Pinilla-Alonso, N., Campins, H., Licandro, L., & Marzo, G. A. (2012) Near-infrared spectroscopic survey of B-type asteroids: Compositional Analysis. *Icarus*, 218, 196.
- De Luise, F., Dotto, E., Fornasier, S., Barucci, M. A., Pinilla-

- Alonso, N., Perna, D. & Marzari, F. (2010) A peculiar family of Jupiter Trojans: The Eurybates. *Icarus*, 209.
- DeMeo, F. E. & Carry, B. (2014) Solar system evolution from compositional mapping of the asteroid belt. *Nature*, 505, 629.
- DeMeo, F. E. & Carry, B. (2013) The taxonomic distribution of asteroids from multi-filter all-sky photometric surveys. *Icarus*, 226, 723.
- de Sanctis, M. C., Migliorini, A., Luzia Jasmim, F., Lazzaro, D., et al. (2011) Spectral and mineralogical characterization of inner main-belt V-type asteroids. *Astron. & Astrophys.*, 533, A77.
- Dohnanyi, J. S. (1969) Collisional Model of Asteroids and Their Debris. *Jour. of Geophys. Research*, 74, 2531.
- Dorossoundiram, A., Barucci, M. A., Fulchignoni, M. & Florczak, M. (1998) Eos family: a spectroscopic study. *Icarus*, 131, 15.
- Dotto, E., Fornasier, S., Barucci, M. A., et al. (2006) The surface composition of Jupiter Trojans: Visible and near-infrared survey of dynamical families. *Icarus*, 183, 420.
- Duffard, R. & Roig, F. (2009) Two new V-type asteroids in the outer Main Belt? *Planetary & Space Sci.*, 57, 229.
- Dunn, T. L., Burbine, T. H., Bottke, W. F., Clark, J. P. (2013) Mineralogies and source regions of near-Earth asteroids. *Icarus*, 222, 273-282.
- Durda, D. D., Bottke, W. F., Nesvorný, D., et al. (2007) Size-frequency distribution of fragments from SPH/N-body simulations of asteroid impacts: Comparison with observed asteroid families. *Icarus*, 186, 498.
- Fieber-Beyer, S. K., Gaffey, M. J., Kelley, M. S., Reddy, V., Reynolds, C. M., Hicks, T. (2011) The Maria asteroid family: genetic relationships and a plausible source of mesosiderites near the 3:1 Kirkwood gap. *Icarus*, 213, 524.
- Fornasier, S., Dotto, E., Marzari, F., et al. (2004) Visible spectroscopic and photometric survey of L5 Trojans: investigation of dynamical families. *Icarus*, 172, 221.
- Fornasier, S., Dotto, E., Hainaut, O., et al. (2007) Visible spectroscopic and photometric survey of Jupiter Trojans: Final results on dynamical families. *Icarus*, 190, 622.
- Gaffey, M. J., Burbine, T. H., Piatek, J. L., et al. (1993) Mineralogical variations within the S-type asteroid class. *Icarus*, 106, 573.
- Gil-Hutton, R., Lazzaro, D. & Benavidez, P. (2007) Polarimetric observations of Hungaria asteroids. *Astron. & Astrophys.*, 468, 1109.
- Gladman, B., Michel, P. & Froeschlé, C. (2000) The Near-Earth Object Population. *Icarus*, 146, 176.
- Gomes, R., Levison, H. F., Tsiganis, K., & Morbidelli, A. (2005) Origin of the cataclysmic Late Heavy Bombardment period of the terrestrial planets *Nature*, 435, 26.
- Grav, T., Mainzer, A. K., Bauer, J., et al. (2012) WISE/NEOWISE observations of the Hilda population: preliminary results. *Astrophys. J.*, 744, 197.
- Hanuš, J., Durech, J., Brož, M., et al. (2011) A study of asteroid pole-latitude distribution based on an extended set of shape models derived by the lightcurve inversion method. *Astron. Astrophys.*, 530, A134.
- Hanuš, J., Brož, M., Durech, J., et al. (2013) An anisotropic distribution of spin vectors in asteroid families. *Astron. Astrophys.*, 559, A134.
- Harris, A. W., Muller, M., Lisse, C. M. and Cheng, A. F. (2009) A survey of Karin cluster asteroids with the Spitzer Space Telescope. *Icarus*, 199, 86.
- Hestroffer, D., Dell'Oro, A., Cellino, A. & Tanga, P. (2010) The Gaia Mission and the Asteroids. *Lect. Notes in Phys.*, 790, 251.
- Hsieh, H. H. & Jewitt, D. J. (2006) A population of comets in the Main Asteroid Belt. *Science*, 312, 561.
- Ishihara, D., Onaka, T., Kataza, H., et al. (2010) The AKARI/IRC mid-infrared all-sky survey. *Astron. & Astrophys.*, 514, 1.
- Ivezić, Ž., Lupton, R. H., Jurić, M. et al. (2002) Color Confirmation of Asteroid Families. *Astron. J.*, 124, 2943.
- Jasmim, F. L., Lazzaro, D., Carvano, J. M. F., Mothé-Diniz, T., and Hasselmann, P. H. (2013) Mineralogical investigation of several Qp asteroids and their relation to the Vesta family. *Astron. Astrophys.*, 552, A85.
- Jedicke, R., Nesvorný, D., Whiteley, R. J., Ivezić, Ž and Jurić, M. (2004) An age-colour relationship for main-belt S-complex asteroids. *Nature*, 429, 275.
- Jewitt, D., Weaver, H., Agarwal, J., Mutchler, M. & Drahus, M. (2010) A recent disruption of the main-belt asteroid P/2010A2. *Nature*, 467, 817.
- Jewitt, D., Weaver, H., Mutchler, M., Larson, S. & Agarwal, J. (2011) Hubble Space Telescope Observations of Main-belt Comet (596) Scheila. *Astrop. J. Lett.*, 733, 4.
- Kasuga, T., Usui, F., Hasegawa, S., et al. (2012) AKARI/AcuA physical studies of the Cybele asteroid family. *Astron. J.*, 143, 141.
- Kohout, T., Gritsevich, M., Grokhovsky, V. I., et al. (2014) Mineralogy, reflectance spectra, and physical properties of the Chelyabinsk LL5 chondrite - Insight into shock-induced changes in asteroid regoliths. *Icarus*, 228, 78.
- Kim, M.-J., Choi, Y.-J., Moon, H.-K., et al. (2014) Rotational properties of the Maria asteroid family. *Astron. J.* 147, 56.
- Kryszczyńska, A., Colas, F., Polińska, M., et al. (2012) Do Slivan states exist in the Flora family? I. Photometric survey of the Flora region. *Astron. & Astrophys.*, 546, A72.
- Lazzaro, D., Mothé-Diniz, T., Carvano, J. M., et al. (1999) The Eunomia Family: A Visible Spectroscopic Survey *Icarus*, 142, 445.
- Lazzaro, D., Angeli, C. A., Carvano, J. M., Mothé-Diniz, T., Duffard, R. & Florczak, M. (2004) S3OS2: the visible spectroscopic survey of 820 asteroids. *Icarus*, 172, 179.
- Lebofsky, L. A., Sykes, M. V., Tedesco, E. F., et al. (1986) A refined 'standard' thermal model for asteroids based on observations of 1 Ceres and 2 Pallas. *Icarus*, 68, 239.
- Lebofsky, L. A. & Spencer, J. R. (1989) Radiometry and a thermal modeling of asteroids. *Asteroids II*, 128.
- Levison, H. F., Bottke, W. F., Gounelle, M., Morbidelli, A., Nesvorný, D., and Tsiganis, K., (2009). Contamination of the asteroid belt by primordial trans-Neptunian objects. *Nature*, 460, 364-366.
- Licandro, J., Hargrove, K., Kelley, M., et al. (2012) 5-14 μm Spitzer spectra of Themis family asteroids. *Astron. & Astrophys.*, 537, A73.
- Mainzer, A. K., Bauer, J., Grav, T., et al. (2011) Preliminary results from NEOWISE: An enhancement to the Wide-field Infrared Survey Explorer for Solar system science *Astrophys. J.*, 731, 53.
- Mainzer, A. K., Bauer, J., Cutri, R. M., et al. (2014) Initial performance of the NEOWISE Reactivation mission *Astrophys. J.*, 792, 30.
- Masiero, J. R., Mainzer, A. K., Grav, T., et al. (2011) Main belt asteroids with WISE/NEOWISE. I. Preliminary albedos and diameters. *Astrophys. J.*, 741, 68.
- Masiero, J. R., Mainzer, A. K., Grav, T., Bauer, J. M. and Jedicke, R. (2012) Revising the age for the Baptistina asteroid family

- using WISE/NEOWISE data. *Astrophys. J.*, 759, 14.
- Masiero, J. R., Mainzer, A. K., Bauer, J. M., Grav, T., Nugent, C. R. and Stevenson, R. (2013) Asteroid family identification using the hierarchical clustering method and WISE/NEOWISE physical properties. *Astrophys. J.*, 770, 7.
- Masiero, J. R., Grav, T., Mainzer, A. K., et al. (2014) Main Belt Asteroids with WISE/NEOWISE: Near-Infrared Albedos. *Astrophys. J.*, 791, 121.
- Mayne, R. G., Sunshine, J. M., McSween, H. Y., Bus, S. J. & McCoy, T. J. (2011) The origin of Vesta's crust: Insights from spectroscopy of the Vestoids. *Icarus*, 214, 147.
- McCord, T. B., Adams, J. B. & Johnson, T. V. (1970) Asteroid Vesta: Spectral Reflectivity and Compositional Implications. *Science*, 168, 1445.
- Mignard, F., Cellino, A., Muinonen, K., et al. (2007) The Gaia Mission: Expected Applications to Asteroid Science. *Earth, Moon & Plan.*, 101, 97.
- Milani, A. (1993) The Trojan asteroid belt: Proper elements, stability, chaos and families. *Cel. Mech. and Dynam. Astron.*, 57, 59.
- Milani, A., Cellino, A., Knežević, Z., Novaković, B., Spoto, F. & Paolicchi, P. (2014) Asteroid families classification: Exploiting very large datasets. *Icarus*, 239, 46.
- Morbidelli, A., Nesvorný, D., Bottke, W.F., Michel, P., Vokrouhlický, D. & Tanga, P. (2003) The shallow magnitude distribution of asteroid families. *Icarus*, 162, 328.
- Moskovitz, N. A., Willman, M., Burbine, T. H., Binzel, R. P. & Bus, S. J. (2010) A spectroscopic comparison of HED meteorites and V-type asteroids in the inner Main Belt. *Icarus*, 208, 773.
- Moskovitz, N. A., Jedicke, R., Gaidos, E., Willman, M., Nesvorný, D., Fevig, R. & Ivezić, Ž. (2008) The distribution of balastic asteroids in the Main Belt. *Icarus*, 198, 77.
- Mothé-Diniz, T. & Carvano, J. M. (2005) 221 Eos: a remnant of a partially differentiated parent body? *Astron. & Astroph.*, 442, 727.
- Mothé-Diniz, T., Roig, F. and Carvano, J. M. (2005) Reanalysis of asteroid families structure through visible spectroscopy *Icarus*, 174, 54.
- Mothé-Diniz, T. Carvano, J. M., Lazzaro, D. (2003) Distribution of taxonomic classes in the main belt asteroids *Icarus*, 162, 10.
- Mothé-Diniz, T. Carvano, J. M., Bus, S. J., Duffard, R. & Burbine, T. H. (2008a) Mineralogical analysis of the Eos family from near-infrared spectra *Icarus*, 195, 277.
- Mothé-Diniz, T. & Nesvorný, D. (2008b) Visible spectroscopy of extremely young asteroid families *Astron. & Astrophys. Letters*, 486, 9.
- Mothé-Diniz, T. & Nesvorný, D. (2008c) Tírela: an unusual asteroid family in the outer main belt. *Astron. & Astrophys.*, 492, 593.
- Murakami, H., Baba, H., Barthel, P., et al., (2007) The Infrared Astronomical Mission AKARI. *Pub. Astron. Soc. Japan*, 59, S369.
- Nathues, A. (2010) Spectral study of the Eunomia asteroid family Part II: The small bodies *Icarus*, 208, 252.
- Nathues, A., Mottola, S., Kaasalainen, M., & Neukum, G. (2005) Spectral study of the Eunomia asteroid family. I. Eunomia. *Icarus*, 175, 452.
- Neese, C., Ed., Asteroid Taxonomy V6.0. EAR-A-5-DDR-TAXONOMY-V6.0. NASA Planetary Data System, 2010.
- Nesvorný, D., Jedicke, R., Whiteley, R.J. and Ivezić, Ž (2005) Evidence for asteroid space weathering from the Sloan Digital Sky Survey *Icarus*, 173, 132.
- Nesvorný, D. (2012) Nesvorný HCM Asteroid Families V 2.0. NASA Planetary Data System, EAR-A-VARGBDT-5-NESVORNYFAM-V2.0.
- Novaković, B., Cellino, A., Knežević, Z. (2011) Families among high-inclination asteroids. *Icarus*, 216, 184.
- Oszkiewicz, D. A., Muinonen, K., Bowell, E., et al. (2011) Online multi-parameter phase-curve fitting and application to a large corpus of asteroid photometric data *Journ. of Quant. Spectro. and Radiative Trans.*, 112, 1919.
- Oszkiewicz, D. A., Bowell, E., Wasserman, L. H., Muinonen, K., Penttilä, A., et al. (2012) Asteroid taxonomic signatures from photometric phase curves. *Icarus*, 219, 283.
- Parker, A., Ivezić, Ž, Jurić, M., Lupton, R., Sekora, M. D. and Kowalski, A. (2008) The size distributions of asteroid families in the SDSS Moving Object Catalog 4. *Icarus*, 198, 138.
- Rayner, J. T., Toomey, D. W., Onaka, P. M., et al. (2003) SpeX: A Medium-Resolution 0.8-5.5 Micron Spectrograph and Imager for the NASA Infrared Telescope Facility. *Pub. of the Astron. Soc. of the Pacific*, 115, 362.
- Reddy, V., Emery, J. P., Gaffey, M. J., Bottke, W. F., Cramer, A. and Kelley, M. S. (2009) Composition of 298 Baptistina: Implications for the K/T impactor link. *Meteor. and Plan. Sci.*, 44, 1917.
- Reddy, V., Carvano, J. M., Lazzaro, D., et al. (2011) Mineralogical characterization of Baptistina asteroid family: Implications for K/T impactor source. *Icarus*, 216, 184.
- Reddy, V., Sanchez, J. A., Bottke, W. F., et al. (2014) Chelyabinsk meteorite explains unusual spectral properties of Baptistina asteroid family. *Icarus*, 237, 116.
- Rivkin, A. S. & Emery, J. P. (2010) Detection of ice and organics on an asteroidal surface. *Nature*, 464, 1322.
- Roig, F., Nesvorný, D., Gil-Hutton, R. & Lazzaro, D. (2008a) V-type asteroids in the middle main belt. *Icarus*, 194, 125.
- Roig, F., Ribeiro, A. O. and Gil-Hutton, R. (2008b) Taxonomy of asteroid families among the Jupiter Trojans: comparison between spectroscopic data and the Sloan Digital Sky Survey colors *Astron. & Astrophys.*, 483, 911.
- Schenk, P., O'Brien, D. P., Marchi, S., et al. (2012) The Geologically Recent Giant Impact Basins at Vesta's South Pole. *Science*, 336, 694.
- Schunová, E., Granvik, M., Jedicke, R., Gronchi, G., Wainscoat, R. & Abe, S. (2012) Searching for the first near-Earth object family. *Icarus*, 220, 1050.
- Slivan, S. M., Binzel, R. P., Crespo da Silva, L. D., et al. (2003) Spin vectors in the Koronis family: comprehensive results from two independent analyses of 213 rotation lightcurves. *Icarus*, 162, 285.
- Slivan, S. M., Binzel, R. P., Kaasalainen, M., et al. (2009) Spin vectors in the Koronis family. II. Additional clustered spins, and one stray. *Icarus*, 200, 514.
- Slivan, S. M., Binzel, R. P., Boroumand, S. C., et al. (2008) Rotation rates in the Koronis family, complete to H11.2 *Icarus*, 195, 226.
- Solontoi, M. R., Hammergren, M., Gyuk, G. & Puckett, A. (2012) AVAST survey 0.4-1.0 μm spectroscopy of igneous asteroids in the inner and middle main belt. *Icarus*, 220, 577.
- Sunshine, J. M., Bus, S. J., McCoy, T. J., Burbine, T. H., Corrigan, C. M. & Binzel, R. P. (2004) High-calcium pyroxene as an indicator of igneous differentiation in asteroids and meteorites. *Meteor. & Plan. Sci.*, 39, 1343.
- Sunshine, J. M., Connolly, H. C., McCoy, T. J., Bus, S. J. & La

- Croix, L. M. (2008) Ancient Asteroids Enriched in Refractory Inclusions. *Science*, 320, 514.
- Szabó, G. M. and Kiss, L. L. (2008) The shape distribution of asteroid families: Evidence for evolution driven by small impacts *Icarus*, 196, 135.
- Thomas, C. A., Rivkin, A. S., Trilling, D. E., Enga, M.-T. & Grier, J. A. (2011) Space weathering of small Koronis family members *Icarus*, 212, 158.
- Thomas, C. A., Trilling, D. E. & Rivkin, A. S. (2012) Space weathering of small Koronis family members in the SDSS Moving Object Catalog. *Icarus*, 219, 505.
- Usui, F., Kuroda, D., Müller, T. G., et al. (2011) Asteroid Catalog Using Akari: AKARI/IRC Mid-Infrared Asteroid Survey. *Pub. of the Astron. Soc. of Japan*, 63, 1117.
- Usui, F., et al. (2015) AKARI infrared spectroscopic observations of asteroids *in prep.*
- Vernazza, P., Birlan, M., Rossi, A., et al. (2006) Physical characterization of the Karin family. *Astron. & Astrophys.*, 460, 945.
- Vernazza, P., Binzel, R. P., Thomas, C. A., et al. (2008) Compositional differences between meteorites and near-Earth asteroids *Nature*, 454, 858.
- Vernazza, P., Binzel, R. P., Rossi, A., Fulchignoni, M. & Birlan, M. (2009) Solar wind as the origin of rapid reddening of asteroid surfaces *Nature*, 458, 993.
- Vernazza, P., Zanda, B., Binzel, R. P., et al. (2014) Multiple and Fast: The accretion of ordinary chondrite parent bodies *Astroph. J.*, 791, 120.
- Vokrouhlický, D., Nesvorný, D. and Bottke, W. F. (2003) The vector alignments of asteroid spins by thermal torques. *Nature*, 425, 147.
- Walsh, K. J., Delbó, M., Bottke, W. F., Vokrouhlický, D., and Lauretta, D. S. (2013) Introducing the Eulalia and new Polana asteroid families: re-assessing primitive asteroid families in the inner Main Belt. *Icarus*, 225, 283-297.
- Walsh, K. J., Morbidelli, A., Raymond, S. N., O'Brien, D. P., & Mandell, A. M. (2012) Populating the asteroid belt from two parent source regions due to the migration of giant planets - "The Grand Tack". *Meteor. & Plan. Sci.*, 47, 1941.
- Warner, B. D., Harris, A. W., Vokrouhlický, D., Nesvorný, D., Bottke, W. F. (2009) Analysis of the Hungaria asteroid population. *Icarus*, 204, 172.
- Weaver, H. A., Stern, S. A., Mutchler, M. J., et al. (2006) Discovery of two new satellites of Pluto. *Nature*, 439, 943.
- Willman, M., Jedicke, R., Nesvorný, D., Moskovitz, N., Ivezić, Ž., Fevig, R. (2008) Redetermination of the space weathering rate using spectra of Iannini asteroid family members. *Icarus*, 195, 663.
- Willman, M., Jedicke, R., Moskovitz, N., Nesvorný, D., Vokrouhlický, D. & Mothé-Diniz, T. (2010) Using the youngest asteroid clusters to constrain the space weathering and gardening rate on S-complex asteroids. *Icarus*, 208, 758.
- York, D. G., Adelman, J., Anderson, J. E. et al. (2000) The Sloan Digital Sky Survey: Technical Summary. *Astron. J.*, 120, 1579.
- Zappala, V., Cellino, A., Farinella, P. & Knezevic, Z. (1990) Asteroid families. I - Identification by hierarchical clustering and reliability assessment. *Astorn. J.*, 100, 2030.
- Zappalà, V., Cellino, A., Dell'Oro, A. & Paolicchi, P. (2002) Physical and Dynamical Properties of Asteroid Families. *Asteroids III*, 619.
- Zellner, B., Tholen, D. J. and Tedesco, E. F., (1985a). The eight-color asteroid survey - results for 589 minor planets. *Icarus*, 61, 355.
- Zellner, B., Thirunagari, A. and Bender, D., (1985b). The large-scale structure of the asteroid belt. *Icarus*, 62, 505-511.
- Ziffer, J., Campins, H., Licandro, J., et al. (2011) Near-infrared spectroscopy of primitive asteroid families *Icarus*, 213, 538.